J. Fluid Mech. (1996), vol. 318, pp. 375–404



# A model of water wave 'horse-shoe' patterns

By VICTOR I. SHRIRA[1], SERGEI I. BADULIN[1] AND CHRISTIAN KHARIF[2]

[1]P. P. Shirshov Institute of Oceanology, Russian Academy of Sciences, 23 Krasikov str., Moscow 117218, Russia

[2]Institut de Recherche sur les Phenomenes Hors Equilibre, Laboratoire Interactions Ocean Atmosphere, 163 Avenue de Luminy — Case 903, 13288 Marseille Cedex 9, France

(Received 25 July 1995 and in revised form 17 December 1995)

The work suggests a simple qualitative model of the wind wave 'horse-shoe' patterns often seen on the sea surface. The model is aimed at explaining the persistent character of the patterns and their specific asymmetric shape. It is based on the idea that the dominant physical processes are quintet resonant interactions, input due to wind and dissipation, which balance each other. These processes are described at the lowest order in nonlinearity. The consideration is confined to the most essential modes: the central (basic) harmonic and two symmetric oblique satellites, the most rapidly growing ones due to the class II instability. The chosen harmonics are phase locked, i.e. all the waves have equal phase velocities in the direction of the basic wave. This fact along with the symmetry of the satellites ensures the quasi-stationary character of the resulting patterns.

Mathematically the model is a set of three coupled ordinary differential equations for the wave amplitudes. It is derived starting with the integro-differential formulation of water wave equations (Zakharov's equation) modified by taking into account small (of order of quartic nonlinearity) non-conservative effects. In the derivation the symmetry properties of the unperturbed Hamiltonian system were used by taking special canonical transformations, which allow one exactly to reduce the Zakharov equation to the model.

The study of system dynamics is focused on its qualitative aspects. It is shown that if the non-conservative effects are neglected one cannot obtain solutions describing persistent asymmetric patterns, but the presence of small non-conservative effects changes drastically the system dynamics at large times. The main new feature is *attractive equilibria*, which are essentially distinct from the conservative ones. For the existence of the attractors a balance between nonlinearity and non-conservative effects is necessary. A wide class of initial configurations evolves to the attractors of the system, providing a likely scenario for the emergence of the long-lived three-dimensional wind wave patterns. The resulting structures reproduce all the main features of the experimentally observed horse-shoe patterns. In particular, the model provides the characteristic 'crescent' shape of the wave fronts oriented forward and the front-back asymmetry of the wave profiles.

## 1. Introduction

The work is motivated by the desire to find a theoretical explanation of a quite common phenomenon seen by everybody on the sea or river surface under the action

of a fresh wind: the so-called *'horse-shoe'* or *'crescent-shaped'* patterns. Despite their common character and easiness of observation quantitative experimental information is rather meagre. We briefly summarize the experimental evidence one can acquire with the unaided eye. The 'horse-shoe' or 'crescent-shaped' patterns:

(i) are easily observed on the sea surface in the presence of a fresh wind at early stages of the wave development;

(ii) occur in the range of short gravity waves and are relatively *long-lived*, i.e. their characteristic time of existence greatly exceeds the wave period;

(iii) are rather steep with sharpened crests and flattened troughs;

(iv) have front-back asymmetry: the front slopes are steeper than the rear ones.

Their most distinct feature is the specific 'horse-shoe' or 'crescent-like' shape of the wave fronts, *always oriented forward.* An idea of how these patterns look in the sea is given by the photographs in figure 1. Similar patterns were also produced in wave tank experiments both in the absence of wind (Su *et al.* 1982; Su 1982; G. Caulliez 1995, personal communication) and in its presence (Kusaba & Mitsuyasu 1986; G. Caulliez 1995, personal communication).

No quantitative field experiment to investigate specifically this phenomenon has yet been carried out and, to our knowledge, no theory explaining it even qualitatively has been developed. The aim of our study is to fill, at least partially, the latter gap.

The first guess was made by Su *et al.* (1982). They supposed that the structures observed in the tank are manifestations of five-wave processes of the type $3 \Rightarrow 2$ (decay of the plane Stokes wave into two oblique satellites) or the class II instability using the term of McLean (1982), who thoroughly investigated numerically the linear stability of the Stokes wave within the exact potential equations. The transverse scale of the class II instability is of the order of the basic wavelength, in contrast to the modulational (or class I) instability which contributes mainly to nearly longitudinal long-wave modulations. This makes the class II instability a very likely candidate to explain the *incipience* of the crescent-shaped wave structures. Nevertheless, this idea has not been checked quantitatively even in tank experiments, although it should be mentioned that Su (1982) provided a strong argument in its support. He reported a good agreement with McLean's predictions of the predominant longitudinal modulational wavelength.

If we accept this hypothesis, then the main questions to be answered are: Why the class II instability should evolve into steady or quasi-steady patterns? What physical mechanisms shape them in such a specific asymmetric manner?

An attempt to find what happens with class II instability at the nonlinear stage was made by Shemer & Stiassnie (1985) and Stiassnie & Shemer (1987), who considered the nonlinear evolution of the three harmonics subjected to the five-wave resonant interaction. They integrated the resulting set of three complex ordinary differential equations and found periodic variations of the wave amplitudes. The class II instability proved to be reversible, when treated as isolated. No steady or quasi-steady patterns were found.

Another hypothesis (Saffman & Yuen 1980; Meiron, Saffman & Yuen 1982, see also Saffman & Yuen 1985) starts from the opposite end. It relates the steady three-dimensional patterns to bifurcations from two-dimensional ones within the family of steady weakly nonlinear solutions. It was noticed that the three-dimensional wave has smaller energy than the Stokes wave of the same steepness. This idea has two principal shortcomings. First, these three-dimensional waves always have symmetric fronts for both weakly nonlinear and exact equations. Second, the three-dimensional steady waves are unstable as are the Stokes ones (no comparative examination of

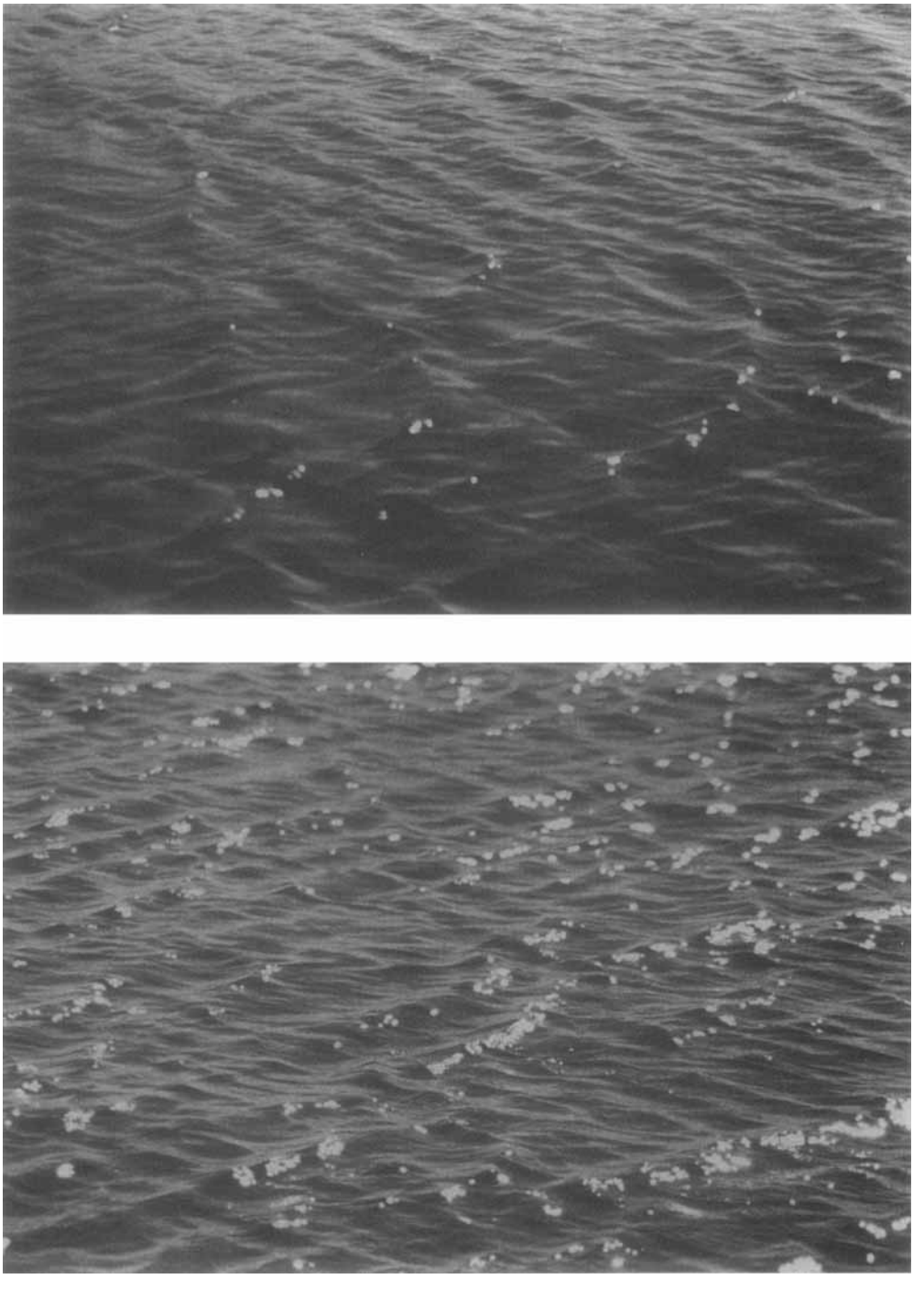

FIGURE 1. Horse-shoe patterns generated by wind in the sea (photo by E. Mollo-Christensen).

instabilities has been carried out yet), therefore their possible role in wave field dynamics remains questionable.

In the present work we study a problem resembling that of Stiassnie & Shemer (1987) based on the Zakharov equation for water waves modified by taking into account non-conservative effects. The use of a new specific technique of canonical transformation applied to the Zakharov equation (see Badulin & Shrira 1996; Badulin *et al.* 1995) enables us to handle the problem analytically. Aiming to explain the phenomenon of the observed 'horse-shoe patterns' we first will investigate the possibility of the appearance of some preferentially stable three-dimensional patterns and, upon getting some success, compare their properties with the experimentally observed ones.

The work is organized as follows. In § 2 starting with the primitive equations and utilizing Zakharov's (1968) approach we arrive at a greatly simplified description for a number of wave modes interacting through four- and five-wave resonances. The selection of the essential modes based upon an analysis of the linear stability problem for the Stokes wave allows us to confine our consideration to just three interacting modes: the Stokes wave itself and two fastest growing symmetric oblique satellites, whose frequencies specified by the class II instability are, in a linear approximation, 3/2 times greater than that of the Stokes wave.

In § 3 we study the Hamiltonian dynamics of such symmetric triads, focusing our attention on the structure of the stationary points of the system. It was found that the system possesses two stationary states corresponding to the essentially three-dimensional wave patterns with two fixed values of the phase difference between the central harmonics and the satellites, namely $\pi n$ and $\pi(n + 1/2)$ ($n$ is integer). We call them *in-phase* and *out-of-phase* states respectively. The in-phase equilibria are identical to those found numerically by Meiron *et al.* (1982); however even the fact of their proved stability in a certain range of wave amplitudes does not make them likely candidates to explain the horse-shoe patterns – their fronts are always symmetric. In the generic case the motion of this Hamiltonian system is periodic. The instantaneous shape of the wave was found to depend mainly on the phase shift between the basic wave and the satellites. In some parts of the trajectories the patterns do resemble the experimentally observed horse-shoes. However it is not possible to freeze the instant: the system passes through these states quite rapidly. Thus, to explain the existence of the persistent structures with curved asymmetric fronts one must go beyond the framework of Hamiltonian dynamics.

In § 4 we consider the dynamics of our triad with non-conservative effects due to wind and dissipation taken into account. The effect of even a small non-conservative perturbation results in qualitative changes in the long-time system behaviour. The elliptic stationary points of the conservative system turn into foci or saddles. The appearance of absolutely attractive foci and slightly unstable saddles can explain the occurrence of the corresponding three-dimensional wave patterns in real situations.

In the Discussion we summarize our conclusions and argue that the stable steady three-dimensional patterns we obtained are indeed the experimentally observed horse-shoes. We also discuss some implementations of the results, as well as the questions raised.

## 2. The model

For the problems our work deals with, the non-conservative effects although small nevertheless play the key role. These non-conservative effects are input due to wind

and wave dissipation due to viscosity and/or sometimes to microbreaking. However a description of particular mechanisms of wave generation and dissipation goes beyond the scope of our work. Fortunately in our context only the most robust facts, just the *presence, sufficient smallness* and *sign* of non-conservative effects proved to be of relevance.

We first concentrate our attention on the conservative dynamics to reveal its inherent limitations and build the basis for the further analysis.

### 2.1. *Basic equations: the Hamiltonian formulation*

Consider potential gravity waves on the free surface of an inviscid, incompressible fluid of infinite depth. The governing equations in the Cartesian frame $\{x, y, z\}$ having the $z = 0$ plane on the undisturbed water surface and the $z$-axis oriented upward are standard:

$$\left.\begin{aligned} &\nabla^2\phi = 0, \quad z \leqslant \eta(x,y,t) \\ &\lim_{z\to-\infty} \nabla\phi = 0, \\ &\left.\begin{aligned} &\phi_t + \eta + \tfrac{1}{2}(\phi_x^2 + \phi_y^2 + \phi_z^2) = 0, \\ &\eta_t + \phi_x\eta_x + \phi_y\eta_y - \phi_z = 0, \end{aligned}\right\} \quad z = \eta(x,y,t), \end{aligned}\right\} \tag{2.1}$$

where $\phi(x, y, z, t)$ is the velocity potential and $z = \eta(x, y, t)$ specifies the free surface; the gravitational acceleration is set to be unity.

We shall deal with the Hamiltonian formulation of the Euler equations of motion (2.1) in Fourier space, proposed by Zakharov (1968). In terms of Fourier amplitudes the complex variables $b(\boldsymbol{k})$ are expressed by means of integral power series in Fourier amplitudes $\eta(\boldsymbol{k})$ and $\psi(\boldsymbol{k})$, free surface elevation and velocity potential at the free surface (see Appendix A). The basic equations (2.1) take the form (asterisk means complex conjugate)

$$\mathrm{i}\frac{\partial b(\boldsymbol{k})}{\partial t} = \frac{\delta H}{\delta b^*(\boldsymbol{k})}, \tag{2.2a}$$

where the Hamiltonian $H$ is expressed in terms of integral power series in complex amplitudes $b(\boldsymbol{k})$:

$$H = H_0 + \sum_{n=4}^{\infty} H_n \tag{2.2b}$$

and

$$H_0 = \int \omega(\boldsymbol{k}) b(\boldsymbol{k}) b^*(\boldsymbol{k}) \mathrm{d}\boldsymbol{k}. \tag{2.2c}$$

Letting the wave amplitudes $b(\boldsymbol{k})$ in series (2.2*b*) be of the order of a small parameter $\varepsilon$, a standard asymptotic approach to the general Hamiltonian equation can be developed in a formal manner. The first term in the expansion of the Hamiltonian $H_0$ being quadratic in $b(\boldsymbol{k})$ gives the linear terms in the equations for $b(\boldsymbol{k})$ ($\omega(\boldsymbol{k})$ is the linear dispersion law). The terms $H_n$ being of power $n$ in amplitudes $b(\boldsymbol{k})$ are responsible for nonlinear terms of order $(n-1)$ in the equations. The procedure for the systematic derivation of the equation was suggested by Zakharov (1968) and improved by Krasitskii (1990, 1994).

Confining ourselves to the first three terms in the series (2.2*b*) we arrive at the

five-wave reduced Zakharov's equation

$$\mathrm{i}\frac{\partial b_0}{\partial t} = \omega_0 b_0 + \int V_{0123} b_1^* b_2 b_3 \delta_{0+1-2-3} \mathrm{d}\boldsymbol{k}_{123} + \int W_{01234} b_1^* b_2 b_3 b_4 \delta_{0+1-2-3-4} \mathrm{d}\boldsymbol{k}_{1234} + \frac{3}{2}\int W_{43210} b_1^* b_2^* b_3 b_4 \delta_{0+1+2-3-4} \mathrm{d}\boldsymbol{k}_{1234}. \tag{2.3}$$

The indices of kernels and $\delta$-functions designate their arguments, e.g. $V_{0123} \equiv V(\boldsymbol{k},\boldsymbol{k}_1,\boldsymbol{k}_2,\boldsymbol{k}_3)$, $\delta_{0+1-2-3} \equiv \delta(\boldsymbol{k}+\boldsymbol{k}_1-\boldsymbol{k}_2-\boldsymbol{k}_3)$. The Hamiltonian five-wave reduced equation (2.3) preserves three basic conservation laws: the Hamilton function $H$ and two components of the momentum (Krasitskii 1994)

$$\boldsymbol{I} = \int \boldsymbol{k} b^*(\boldsymbol{k}) b(\boldsymbol{k}) \mathrm{d}\boldsymbol{k}. \tag{2.4}$$

We look for the solutions to the set of integro-differential equations (2.3) using the following trick (Badulin & Shrira 1996). There is a certain freedom in kernels $V_{0123}$, $W_{01234}$ and in the corresponding canonical transformation to variables $b(\boldsymbol{k})$ allowing one to add an arbitrary function to the kernels obeying the symmetries and vanishing at the resonant curves. The solutions in physical variables remain the same. This enables one to simplify the equations and get the exact solutions to them in an extremely simple form, namely in the form of the superposition of a number of $\delta$-pulses in the wavevector space

$$b(\boldsymbol{k}) = \sum_{i=0}^{N} b_i(t)\delta(\boldsymbol{k}-\boldsymbol{k}_i). \tag{2.5}$$

Here $b_i(t)$, $\boldsymbol{k}_i$ are amplitudes and wavevectors of fixed harmonics. In this case the integro-differential equation (2.3) exactly reduces to a set of $N$ ordinary differential equations (ODEs) for the complex amplitudes of modes $b_i(t)$. The key point in the construction of this set of $N$ equations is that the $N$ modes of (2.5) constitute an *isolated system* of four- and five-wave resonances (see Badulin & Shrira 1996). The term 'isolated' means here that there are no harmonics $\boldsymbol{K}$ which are in approximate four- or five-wave resonances with harmonics $\boldsymbol{k}_i$ of the ansatz (2.5), i.e. $\boldsymbol{K}$ satisfying the following two sets of equations

$$\boldsymbol{K} = \sum_1^3 s_j \boldsymbol{k}_j, \quad \omega(\boldsymbol{K}) = \sum_1^3 s_j \omega(\boldsymbol{k}_j) + O(\varepsilon^3), \tag{2.6a}$$

$$\boldsymbol{K} = \sum_1^4 s_j \boldsymbol{k}_j, \quad \omega(\boldsymbol{K}) = \sum_1^4 s_j \omega(\boldsymbol{k}_j) + O(\varepsilon^3). \tag{2.6b}$$

Here wavevectors $\boldsymbol{k}_j$ with different $j$ can be equivalent and $s_j = \pm 1$. Provided there is no $\boldsymbol{K}$ satisfying the above system, the ansatz (2.5) is an exact solution of the reduced Zakharov equation. The evolution of the modes is described by a set of $N$ ordinary differential equations.

The procedure of construction of such exact solutions of the reduced Zakharov equation (2.3) can be summarized as follows (see Badulin & Shrira 1996). Starting with the initial conditions in the form (2.5) we require amplitudes $b(\boldsymbol{K})$ of all possible combinations of the basic wavevectors $\boldsymbol{k}_j$ (2.6*a*,*b*) to remain plain zeros. These

conditions mean the zeroing of the corresponding kernels $V_{0123}$ and $W_{01234}$. Owing to the above mentioned freedom these kernels are fixed only at the resonant curves and can be chosen arbitrarily outside these curves (provided the necessary symmetries are kept). Thus, we put the kernels for non-resonant harmonics $\boldsymbol{K}$ equal to zero by a proper choice of canonical transformation. This canonical transformation has to be sufficiently smooth within the weakly nonlinear paradigm, which requires wavevectors $\boldsymbol{K}$ to lie outside some proximity of the resonant curves – 'resonant zones'.

We note that only due to the 'technical' trick described above, which allowed us to get the exact solution in the extremely simple form, does the problem becomes tractable analytically without the use of symbolic manipulators. For example, the ansatz (2.5) for, say, just three delta-functions corresponds to 66 (!) items in terms of the Fourier modes of the original variables $\phi$ and $\eta$. For some applications lying beyond the immediate scope of this work it is also important that the adopted approach enables us to describe the wave field with accuracy up to the quartic terms, while the models used previously (Shemer & Stiassnie 1985; Stiassnie & Shemer 1987) do not describe properly the cubic terms of the solution and do not preserve the energy integral with this accuracy.

### 2.2. *Selection of the dominant resonant processes*

Being interested in the three-dimensional structures emerging from plane waves, consider first the available knowledge on the instability of a plane wave with respect to small perturbations (McLean *et al.* 1981; Craik 1986). A plane wave with a wavevector, say, $\boldsymbol{k}_a$ is unstable with respect to perturbations having wavevectors $\boldsymbol{k}_b$, $\boldsymbol{k}_c$ which obey approximately a resonance condition

$$n\boldsymbol{k}_a = \boldsymbol{k}_b + \boldsymbol{k}_c, \quad n\omega_a = \omega_b + \omega_c, \tag{2.7}$$

where integer $n = 2,3,4,\ldots$ corresponds to quartet, quintet, sextet etc. resonant interactions having $O(\varepsilon^{-n})$ characteristic timescales. Strictly speaking, in the generic case to describe the evolution of the instability emerging from a Stokes' wave with a superimposed noise one should deal with a continuum of coupled harmonics having in common the central (basic) harmonics which obey (2.7). Moreover, at the nonlinear stage of evolution one should take into account all the interactions among the harmonics generated or enhanced by the instabilities, which makes the problem tractable only via an extensive direct numerical simulation.

To get an analytically feasible model we make an assumption which radically simplifies the problem. As is common in the theory of hydrodynamic stability we consider the evolution of a system composed of a minimal, in this context, number of harmonics: the basic wave and two modes corresponding to the fastest growing transversal perturbations. The physical arguments in support of the adequacy of such a model for the study of the pattern formation can be summarized as follows.

The lowest-order instability of the plane deep water wave due to four-wave interactions (the Benjamin–Feir instability) is nearly one-dimensional and is confined to relatively large spatial scales of order $\varepsilon^{-1}$. Obviously this process cannot be the dominant one in the formation of the three-dimensional patterns under consideration. The essentially transverse instabilities with the dominant scale of order of the basic wavelength appear owing to the five-wave and higher-order interactions. The instability domains in wavevector space due to these interactions are very narrow, generally $O(\varepsilon^n)$. They have maximal width for the transversally symmetric wavevector configurations. This is a purely kinematic fact caused by vanishing of the corresponding derivatives of the group velocities. The maximal growth rates of linear

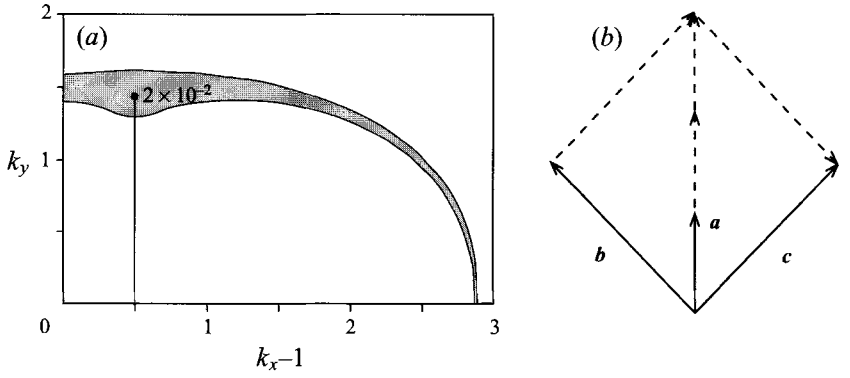


FIGURE 2. Selection of the dominant triad. (*a*) Instability rate diagram for the Stokes wave of steepness 0.3. (*b*) The dominant symmetric resonant triad in $\boldsymbol{k}$-space.

instability correspond to these symmetric patterns as well (McLean 1982; Kharif & Ramamonjiarisoa 1990). Their remarkable feature ensuring the possibility of a quasi-permanent form of the resulting patterns is that these perturbations are *phase locked* with the basic wave, i.e. they move with the same celerity as the basic wave while having standing-wave structure in the transverse direction.

Weakly nonlinear theory predicts instability rates of the order of $\varepsilon^n$. Thus it is natural to restrict our consideration to the lowest, the fifth-order, resonances of the type (2.7) with $n = 3$, which leads to the approximate ($\varepsilon \to 0$) resonance conditions

$$\omega_b = (\tfrac{3}{2})\omega_a, \qquad k_{bx} = (\tfrac{3}{2})k_{ax}, \qquad k_{by} = (\tfrac{3}{4})\sqrt{5}k_{ay}. \tag{2.8}$$

We also note that for steepness exceeding 0.3 the maximal rates of the class II instability exceed Benjamin–Feir instability rates and thus for steep waves the five-wave instability becomes the dominant process (see McLean 1982; Kharif & Ramamonjiarisoa 1990). An illustration of the location of instability domains in $\boldsymbol{k}$-space for this threshold steepness 0.3 is given in figure 2. The arguments above show an exceptional feature of transversally symmetric configurations. They enable one to expect their dominance at the nonlinear stages of the wave-field evolution as well.

### 2.3. *Three-mode equations*

#### 2.3.1. *Hamiltonian equations*

Consider a three-phase wave system (2.5) which is in five-wave resonance (2.7), with $n = 3$. Without additional approximations we get the following set of three ordinary differential equations for complex amplitudes of these modes, $a, b, c$, respectively:

$$\left.\begin{aligned} \mathrm{i}a_t &= \omega_a a + [V_{aaaa}|a|^2 + 2V_{abab}|b|^2 + 2V_{acac}|c|^2]a + 3W_{bcaaa}bc(a^2)^*, \\ \mathrm{i}b_t &= \omega_b b + [2V_{abab}|a|^2 + V_{bbbb}|b|^2 + 2V_{bcbc}|c|^2]b + W_{bcaaa}b^*a^3, \\ \mathrm{i}c_t &= \omega_c c + [2V_{acac}|a|^2 + 2V_{bcbc}|b|^2 + V_{cccc}|c|^2]c + W_{bcaaa}c^*a^3. \end{aligned}\right\} \tag{2.9}$$

The so-called 'natural symmetry' conditions of kernels $V$, $W$ are used here (see Krasitskii 1994). The set (2.9) corresponds exactly to the general Hamiltonian equation (2.3) and therefore it has the same basic laws of conservation of energy and momentum of our wave pattern. The conservation of the two components of momentum yields

$$|a|^2 + \tfrac{3}{2}(|b|^2 + |c|^2) = I_1, \quad \tfrac{3}{2}(|b|^2 - |c|^2) = I_2, \tag{2.10}$$

where for $I_1$ we have used the form symmetric in $b$ and $c$.

Performing the transformation to real amplitudes and phases

$$a = A\exp(-\mathrm{i}\alpha), \quad b = B\exp(-\mathrm{i}\beta), \quad c = C\exp(-\mathrm{i}\gamma), \tag{2.11}$$

we reduce equations (2.9) to four equations for the real amplitudes $A$, $B$, $C$ and the phase $\Phi$:

$$\left.\begin{aligned} A_t &= 3W_{bcaaa}BCA^2\sin\Phi, \\ B_t &= -W_{bcaaa}CA^3\sin\Phi, \\ C_t &= -W_{bcaaa}BA^3\sin\Phi, \\ \Phi_t &= 3\Omega_a - \Omega_b - \Omega_c + W_{bcaaa}\left(9ABC - \frac{A^3B}{C} - \frac{A^3C}{B}\right)\cos\Phi, \end{aligned}\right\} \tag{2.12a}$$

where

$$\Phi = 3\alpha - \beta - \gamma, \tag{2.12b}$$

$$\left.\begin{aligned} \Omega_a &= \omega_a + V_{aaaa}A^2 + 2V_{abab}B^2 + 2V_{acac}C^2, \\ \Omega_b &= \omega_b + 2V_{abab}A^2 + V_{bbbb}B^2 + 2V_{bcbc}C^2, \\ \Omega_c &= \omega_c + 2V_{acac}A^2 + 2V_{bcbc}B^2 + V_{cccc}C^2. \end{aligned}\right\} \tag{2.12c}$$

The first integral of the system – the Hamiltonian – takes the form

$$\begin{aligned} H &= \omega_aA^2 + \omega_bB^2 + \omega_cC^2 \\ &\quad + (V_{aaaa}A^4 + V_{bbbb}B^4 + V_{cccc}C^4 + 4V_{abab}A^2B^2 + 4V_{acac}A^2C^2 + 4V_{bcbc}B^2C^2)/2 \\ &\quad + 6A^3BCW_{bcaaa}\cos\Phi. \end{aligned} \tag{2.13}$$

The system can be easily reduced to a single ordinary differential equation by using the three conservation laws (2.10), (2.13) and, thus, be integrated (see Shemer & Stiassnie 1985).

Bearing in mind the speculations of the previous subsection on the possible mode selection in multi-phase wave systems, we consider further the transversally symmetric three-wave patterns only, namely we put amplitudes and phases of the satellites equal, i.e. $B = C$, $\beta = \gamma$. This results immediately (2.10), (2.12*a*), (2.13) in the very simple conservation laws

$$\tfrac{1}{2}(B^2 - C^2) = I_2 = 0, \quad A^2 + 3B^2 = I_1 = I \tag{2.14}$$

and the governing equations in real variables in the form

$$\left.\begin{aligned} A_t &= W_{bcaaa}(I - A^2)A^2\sin\Phi, \\ \Phi_t &= \delta + MA^2 + W_{bcaaa}A(3I - 5A^2)\cos\Phi, \end{aligned}\right\} \tag{2.15}$$

where the phase $\Phi$ is now defined as

$$\Phi = 3\alpha - 2\beta. \tag{2.16a}$$

The parameter $\delta$, defined as

$$\delta = 3\omega_a - 2\omega_b + I[(12V_{abab} - 2V_{bbbb} - 4V_{bcbc})/3], \tag{2.16b}$$

can be interpreted as the frequency shift due to linear frequencies mismatch and the constant part of the nonlinear frequency shift (in square brackets). The parameter $M$

$$M = 3V_{aaaa} - 8V_{abab} + \tfrac{2}{3}V_{bbbb} + \tfrac{4}{3}V_{bcbc}, \tag{2.16c}$$

is the coefficient responsible for the nonlinear frequency modulation. The interaction coefficient $W_{bcaaa}$ will be designated as $W$ for brevity; the explicit expressions for $V, W$ are given in Krasitskii (1994), Badulin *et al.* (1995). The first integral of the system, the Hamiltonian, now takes the form (cf. (2.13))

$$H = \delta A^2 + MA^4/2 + 2W(I - A^2)A^3 \cos \Phi. \tag{2.17}$$

Thus, the system (2.15) being an easy target for complete analysis provides a good starting point for understanding of much more sophisticated non-conservative dynamics.

2.3.2. *Weakly non-conservative equations*

The dynamics of wind waves is not entirely Hamiltonian: the non-conservative effects of wind, viscous dissipation and other factors can strongly affect wave field evolution. Unfortunately, there is no clarity yet in the physics of wave generation. Even for two-dimensional small-amplitude waves there are a number of competing theories based on quite different approaches (see e.g. Miles 1994; Belcher & Hunt 1993). For the steep three-dimensional waves we are concerned with there is no theory, numerical simulation or laboratory experiment. The situation is even worse with the understanding of the numerous mechanisms of wave dissipation. However, any analysis of physical mechanisms of wave dissipation/generation goes beyond the scope of this work. We shall adopt the following approach. We assume that energy input and sink do occur in the system under consideration, being of the order of the quartic nonlinear terms, i.e. of order $\varepsilon^4$ and shall focus our study on the fundamental aspects of the dynamics which do not depend or depend only very weakly on the specific features of the non-conservative terms.

There are rather obvious grounds to take non-conservative effects of order $\varepsilon^4$. The smaller effects become important only at much larger timescales; stronger effects will prevail and make the nonlinear wave interactions negligible. It should be also mentioned that the chosen scaling does not contradict available experimental evidence. To take into account weak non-conservative effects in a systematic manner one should perform an asymptotic procedure in powers of $\varepsilon$ quite similar to that we performed for the conservative problem. The results can be easily anticipated if we let the linear dispersive law have a small imaginary part, that is

$$\omega = \omega_a(1 + \mathrm{i}\gamma_a); \qquad \Gamma_a = \omega_a\gamma_a; \qquad \gamma_a \approx O(\varepsilon^3). \tag{2.18}$$

Negative $\gamma_a$ ($\Gamma_a$) corresponds to dissipation and positive to generation of a harmonic. In generic situations any asymptotic expansion in wave amplitudes in the equations yields linear non-conservative term at the leading order. In principle we can allow generation and dissipation to depend on the wave amplitudes; however, having no well established theory for choosing the right nonlinear dissipation and generation we confine ourselves to the simplest case of linear dissipation and generation, i.e. to constant $\gamma$. Recall that constant $\gamma$ corresponds to the generic situation. The fact that the non-conservative effects are of order $\varepsilon^4$ means that they enter $O(\varepsilon^4)$ dynamic equations in the additive way.

In particular, for the case of symmetric three-mode wave patterns we are interested in, we get

$$\left.\begin{aligned} A_t &= 3WB^2A^2 \sin(\Phi + \gamma_a) + \Gamma_a A, \\ B_t &= -WBA^3 \sin(\Phi - \gamma_b) + \Gamma_b B, \\ \Phi_t &= 3\Omega_a - 2\Omega_b + W[9AB^2 \cos(\Phi + \gamma_a) - 2A^3 \cos(\Phi - \gamma_b)]. \end{aligned}\right\} \tag{2.19}$$

These equations provide the framework for our further consideration.

The essence of this section can be summarized as follows. All the assumptions made by now are embodied in equations (2.19). These equations constitute the mathematical model of the phenomenon under consideration. The model is based on the idea that the main processes are the quintet resonant interactions and input and dissipation due to wind and other factors. These processes are taken into account at the lowest possible order. Obviously being not identical to the very complex phenomenon of horse-shoe pattern formation, the model, as we show below, does describe some of its essential features.

## 3. Hamiltonian dynamics of the transversally symmetric triad

The system (2.12*a*) can be easily integrated and all the desired properties of the solutions surely could be readily found in this manner (see Shemer & Stiassnie 1985). However the investigation of this system in itself is not the goal of our study: we need it just to provide the basis for the analysis of the more complex non-conservative system.

First we note that in the Hamilton function (2.17) there are terms of three different orders in amplitude. Taking into account all orders in the Hamiltonian becomes of over-riding importance when the sum of the two lowest-order terms is close to zero. In this case the highest-order term can give new physical effects. In the space of parameters $I, \delta$ there are always domains where this balance holds. We recall that $\delta$ measures the mismatch between the frequencies while $I$ roughly characterizes the nonlinearity of the problem.

The basic equations for three-wave patterns (2.12*a*,*b*,*c*) and their symmetric simplifications (2.15) resemble those of the classical problem of three-wave interactions (see Weiland & Wilhelmsson 1977; Craik 1986). The comparison of these systems is useful to carry out in terms of an analogy with the motion of a particle in a potential field. On using the conservation laws these systems (see Weiland & Wilhelmsson 1977, chapter 9) can be transformed into the form of a single second-order differential equation, quite similar to the Newton equation for a particle in a one-dimensional potential field

$$\frac{\mathrm{d}^2 A}{\mathrm{d}t^2} = -\frac{\partial \Pi_m(A)}{\partial A}, \tag{3.1}$$

where the amplitude $A$ becomes an analogue of the particle coordinate, and the order $m$ of the polynomial $\Pi_m$ equals the order of wave interaction ($m = 3$ for three-wave interactions, $m = 5$ for the problem under consideration). The total energy of the particle is constant, that is

$$E = \left(\frac{\mathrm{d}A}{\mathrm{d}t}\right)^2 + \Pi_m(A).$$

Depending on the initial total energy (or equivalently, on the initial wave amplitude) a number of stationary points (stable and unstable) can exist (see figure 3). In the case of the classical triad interactions we have no more than two stationary points, while in our case of five-wave interactions we can get four stationary points. Thus, there are grounds to expect essentially richer dynamics in our problem than in the classical three-wave one.

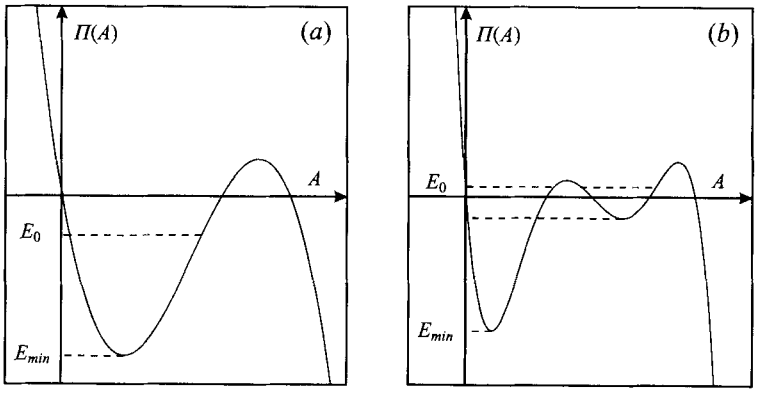


FIGURE 3. Wave pattern conservative dynamics in terms of particle motion in a potential field. (*a*) Three-wave resonant interactions. The potential energy $\Pi(A)$ is a cubic polynomial, two stationary points are possible. The particle motion occurs on the surfaces of constant total energy $E_0$. (*b*) Five-wave interaction potential. $\Pi(A)$ is a fifth-order polynomial. There are four stationary points and two finite regimes of motion are possible for the same energy level $E_0$.

### 3.1. *Stationary states*

#### 3.1.1. *'Trivial' stationary states*

We start our analysis with the study of the simplest stationary states of the system (2.15) corresponding to zero amplitude of one of the harmonics. We shall call these states *trivial*. They include:

(*a*) the short-crested wave

$$A_0 = 0, \qquad B_0^2 = I/3, \qquad \delta = 0; \tag{3.2a}$$

(*b*) the plane Stokes wave

$$A_0^2 = I, \qquad B_0 = 0, \qquad \delta + MA_0^2 - 2WA_0^3 \cos\Phi_0 = 0. \tag{3.2b}$$

Here the subscript 0 is used to designate the equilibrium parameters. We note that within the classical three-wave interactions (Craik 1986) there is no analogue of the short-crested wave state (3.2*a*). As can be easily shown, the short-crested stationary waves we found are neutrally stable in the linear approximation, that is the corresponding linear stability problem is degenerate (all eigenvalues are plain zeros). For this state to occur certain conditions on the frequency mismatch should be satisfied, while there are no limitations on the phase shift $\Phi_0$.

The second stationary state (3.2*b*) is the well-known Stokes plane wave. The evolution of infinitely small perturbations of amplitude $B$ for this state depends on the phase $\Phi$. It is easy to show that for

$$\Phi_0 = m\pi, \qquad m = 0, \pm 1, \pm 2 \ldots$$

this stationary point is neutrally stable; for all other values of $\Phi_0$ this state is unstable. The maximal growth rates are in agreement with the predictions of linear instability analysis (McLean *et al.* 1981; Zakharov 1968) and correspond to the extrema of the Hamilton function (total energy) (2.17).

#### 3.1.2. *Non-trivial essentially three-dimensional stationary states*

We shall call essentially three-dimensional stationary points with non-zero amplitudes $A_0$ and $B_0$ *'non-trivial states'*. For these states to exist we have the necessary

condition in terms of the phase $\Phi_0$,

$$\sin \Phi_0 = 0.$$

Depending on the amplitude $A_0$, two types of equilibria are possible:

(*a*) *'in-phase'* states

$$\delta + MA_0^2 + WA_0(3I - 5A_0^2) = 0, \qquad \Phi_0 = \pm 2m\pi; \tag{3.3a}$$

(*b*) *'out-of-phase'* states

$$\delta + MA_0^2 - WA_0(3I - 5A_0^2) = 0, \qquad \Phi_0 = \pm(2m+1)\pi, \tag{3.3b}$$

where $m$ is an arbitrary integer. We introduce the terms '*in-phase*' and '*out-of-phase*' because from the definition of $\Phi$ (2.16*a*), $\Phi \equiv 3\alpha - 2\beta$, it follows that the corresponding phase shifts between the central harmonic and the satellites, i.e. $\beta$, are $(m\pi)$ and $(m\pi + \pi/2)$.

The equilibria (3.3*a*) are identical to those found numerically by Meiron *et al.* (1982) within the exact equations, while another family (3.3*b*) is new, to our knowledge.

Within the framework of our equations the analysis of the stability of these equilibria is straightforward. Linearizing (2.15) about equilibrium the (3.3*a*) and using the evident inequality $I \geqslant A_0^2$ (see 2.10) we obtain a simple stability criterion for the 'in-phase' equilibria,

$$2MA_0^2 + WA_0(3I - 15A_0^2) < 0.$$

This condition can be easily satisfied for any small $I$ (that is for any small wave steepness) by a proper choice of the mismatch parameter $\delta$.

Similarly obtained, the stability criteria for the 'out-of-phase' stationary states (3.3*b*)

$$2MA_0^2 - WA_0(3I - 15A_0^2) > 0$$

can be satisfied for very steep waves only (the steepness should exceed $\simeq 0.7$).

We pay particular attention to the elliptic stationary points of the conservative problem, as one can expect a transformation of these states into stable or unstable foci when weak non-conservative effects are taken into account. For small and moderate wave amplitudes we find only one type of stationary point (3.3*a*). The second stationary point (3.3*b*) appears at wave steepness exceeding the extreme values for the Stokes deep water waves. It should be noted however that generally three-dimensional waves usually have much higher extreme steepness and Zakharov's equation even with only cubic terms retained, describes them with a good accuracy up to steepness $\simeq 0.4$ (see Badulin *et al.* 1995).

It is important to note that both the 'in-phase' and 'out-of-phase' equilibria we have found are non-isolated, i.e. the condition of stationarity prescribes a curve in the phase space

$$\sin \Phi_0 = 0, \qquad f(A_0, B_0) = 0.$$

This indicates that the system is structurally unstable with respect to a small non-conservative perturbation. In particular, we show below that new stable equilibria can appear at much lower values of wave steepness.

### 3.2. *Discussion: Hamiltonian dynamics of the triad*

Let us formulate again, now in terms of the chosen three-mode system, the requirements of a theory attempting to explain the basic experimental evidence on horse-shoe patterns and consider from this viewpoint the Hamiltonian dynamics of the triad.

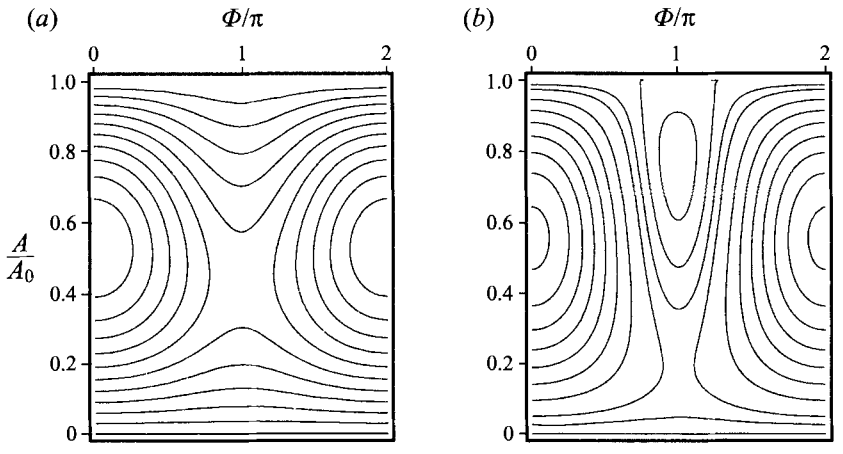


FIGURE 4. Phase portraits of the system (2.15) for different values of wave steepness. (*a*) $\varepsilon = 0.25$: elliptic stationary point at $\Phi = 0$ and hyperbolic point at $\Phi = \pi$. (*b*) $\varepsilon = 0.75$: two elliptic stationary points at $\Phi = 0$ and $\Phi = \pi$.

A theory must explain at least two main points: (i) the emergence of long-lived three-dimensional patterns from the instability of a Stokes's wave. This means that there should be trajectories which begin in the vicinity of trivial equilibria corresponding to the Stokes wave and reach a stable equilibrium; (ii) the characteristic asymmetric crescent fronts and their permanent orientation forward, which means that the equilibrium should have a fixed value of phase $\Phi_0$ lying within the interval $[-\pi, 0]$.

A good idea of the dynamics of the triad could be acquired from the analysis of phase plane of the system. Some examples of phase portraits of system (2.15) for different values of governing parameters $\delta$ and $A_0^2/I$ ($A_0$ is an initial wave amplitude which is proportional at the leading order in $\varepsilon$ to wave steepness) are shown in figure 4. Being primarily interested in the nonlinear stage of the McLean instability of the plane waves, we can see in figure 4 that the trajectories originating in the vicinity of the unstable stationary point ($A = A_0, B_0 = 0$) are always periodic and, unless the initial deviation from the plane wave is large enough, the phase $\Phi$ inevitably varies from 0 to $2\pi$. It is clear that within this conservative problem there is no way for the system to start in the vicinity of the plane wave and reach a stable equilibrium. The shape of the wave patterns corresponding to different points in a trajectory depends mainly on $\Phi$.

To illustrate this point some samples of the patterns taken along one typical trajectory are depicted in figure 5. While at some phases the resulting patterns do resemble the horse-shoe ones, they pass through these states pretty quickly. We note that the system could stay for a quite a long time in the vicinity of the saddle point. However these states are not the ones we are looking for, as they are structurally unstable and symmetric, contrary to the observations.

Thus, it does not seem possible to explain the existence of persistent asymmetric patterns within the framework of purely Hamiltonian dynamics.

## 4. Weakly non-conservative three-dimensional patterns

### 4.1. *Equilibria of the non-conservative system*

We continue our line of study by focusing attention on the stationary states of the system. The 'non-conservative' equilibria are specified by the set of equations (2.19)

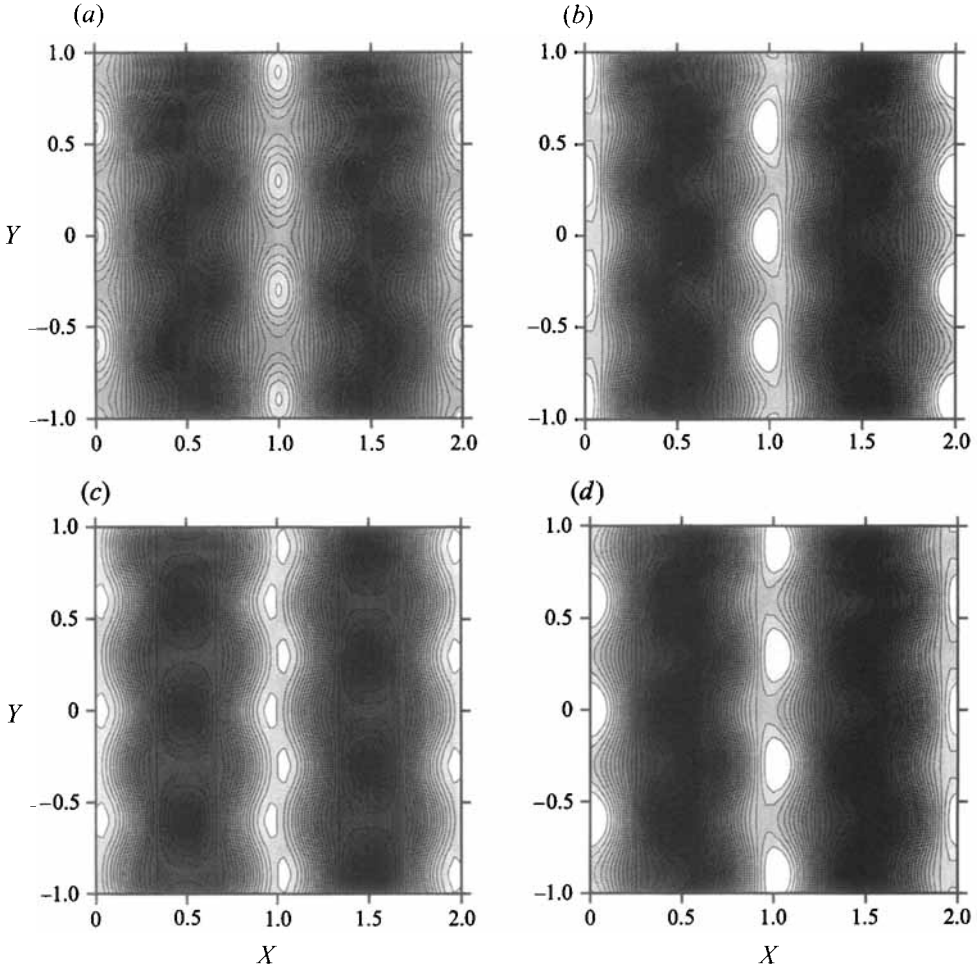


FIGURE 5. Samples of the three-dimensional wave patterns along a trajectory of figure 4 taken at different moments of time. Waves propagate rightward. (Maxima are white, minima are black.) The amplitude of the initial perturbation is 15% of the basic wave. (*a*) $\Phi = 0$ , (*b*) $\Phi = \pi/2$, (*c*) $\Phi = \pi$, (*d*) $\Phi = 3\pi/2$.

with the left-hand side put to zero. These equations prescribe the 'equilibrium' values of the amplitudes $A_0$, $B_0$ and the phase $\Phi_0$ as functions of 'external' parameters of generation/dissipation $\Gamma_a, \Gamma_b$ and the linear frequency mismatch $\delta$ specifying the chosen triad.

The set of equations (2.19) is greatly simplified by expanding in $\gamma$ and retaining the leading-order terms. Letting formally $\gamma_a = 0$, $\gamma_b = 0$ in the argument of the sine in (2.19) in the case of finite $\Phi_0$ we have

$$3WB_0^2A_0^2 \sin\Phi_0 + \Gamma_a A_0 = 0, \quad -WB_0A_0^3 \sin\Phi_0 + \Gamma_b B_0 = 0. \tag{4.1}$$

We omitted the equation for the phase $\Phi_0$ which can be assumed automatically satisfied, say by a proper choice of the linear frequency mismatch. Consider some conjectures that one can immediately see from equations (4.1).

(*a*) For the existence of an equilibrium it is necessary for the system to have a balance between energy input and dissipation. This implies the condition

$$\Gamma_a\Gamma_b < 0, \tag{4.2}$$

which means that either energy input into central harmonics is balanced by the dissipation of satellites or vice versa.

(*b*) The 'trivial' equilibria (3.2*a*,*b*) disappear, i.e. the stationary plane wave and short-crested wave patterns are not possible in the non-conservative system. This important fact has the same general physical basis. While any stationary state in the non-conservative system needs a balance of generation and dissipation, the zero amplitude of one of the harmonics means the absence of either the energy input or sink, thus forcing the former 'trivial' stationary states either to grow or to decay.

(*c*) The ratio of the amplitudes of the satellites to the central harmonics is fixed by the simple relation

$$-\frac{\Gamma_a}{\Gamma_b} = \frac{3B_0^2}{A_0^2} \equiv R. \tag{4.3}$$

We emphasize that this parameter of the stationary states is prescribed exclusively by the ratio of the system input/output.

(*d*) The non-conservative equilibria are essentially distinct from their conservative counterparts. While the conservative stationary points could have just two fixed values (zero and $\pi$) of the phase $\Phi$, the phases of the non-conservative equilibria fill all the interval $[0, 2\pi]$.

Below we consider some properties of these equilibria in more detail, focusing on the two most interesting limiting cases: that of the infinitesimal non-conservative effects and that of the 'maximal possible' ones. The latter class of equilibria will be referred to as *'saturated states'*.

### 4.1.1. *Infinitesimal dissipation/generation*

We are particularly interested to trace the relations between the 'non-conservative' and Hamiltonian equilibria. To understand the role of non-conservative perturbations in the system dynamics we start with the case of infinitesimal dissipation/generation. We shall refer to the dissipation as *very weak* if it is small compared to the quartic nonlinearity. This means the scaling

$$\Gamma \ll W\varepsilon^3 \sim WI^{3/2}. \tag{4.4}$$

Using the scaling (4.4) we easily find the approximate formulae for $\Phi_0$ for the equilibria of the system (2.19):

$$\Phi_0 = -\Gamma_a\left(\omega_a^{-1} + \frac{1}{3WA_0B_0^2}\right) = \Gamma_b\left(\omega_b^{-1} + \frac{1}{WA_0^3}\right), \tag{4.5a}$$

$$\Phi_0 = \pi + \Gamma_a\left(\omega_a^{-1} + \frac{1}{3WA_0B_0^2}\right) = \pi - \Gamma_b\left(\omega_b^{-1} + \frac{1}{WA_0^3}\right). \tag{4.5b}$$

For the stationary amplitudes we arrive again at the approximate formula (4.3). We stress that the trivial stationary states (plane and short-crested waves (3.2*a*,*b*)) are structurally unstable with respect to any infinitely small non-conservative perturbations, i.e. they disappear as soon as any infinitely small dissipation/generation terms are incorporated into our dynamical model (2.19).

The question of the modification of the non-trivial stationary states due to small non-conservative factors is not so simple as the previous one. The shift of stationary points in phase $\Phi_0$ relative to the conservative problem is negligibly small (in that the dissipation is very weak in the sense (4.4)), but the amplitudes corresponding to these stationary points change drastically. These changes are due to the disappearance of

the conservative integrals of motion. As we consider the ultimate states of the system, the non-conservative system 'forgets' its initial 'conservative' parameters. The small effect being accumulated over a long period of time results in considerable changes in the stationary states. From the equation for the phase $\Phi_0$ and (4.5*a*,*b*) we have for the stationary points ($\Phi_0$ is small)

$$\delta_{nc} + M_{nc}A_0^2 \pm WA_0^3(9R - 2) = 0, \tag{4.6}$$

where the mismatch $\delta_{nc}$ is expressed in terms of linear frequencies of harmonics

$$\delta_{nc} = 3\omega_a - 2\omega_b$$

and the modulational parameter is

$$M_{nc} = 3V_{aaaa} - 8V_{abab} + R(10V_{abab} - 8V_{bcbc} - 2V_{bbbb}).$$

Subscript *nc* for 'non-conservative' values of parameters $\delta_{nc}$ and $M_{nc}$ is introduced to emphasize the fact that their values differ from those of the 'conservative' problem (3.3*a*,*b*). We can trace the links of these non-trivial stationary states in the conservative and the non-conservative problem in terms of specific 'in-phase' and 'out-of-phase' patterns of water waves as the changes in $\Phi_0$ remain small. At the same time, we recall again that the values of the stationary amplitudes $A_0$ and $B_0$ significantly change relative to their 'conservative' counterparts regardless of the smallness of the generation/dissipation. As we show below, these displacements of equilibria strongly change the stability properties of these 'in-phase' and 'out-of-phase' patterns.

4.1.2. *'Saturated' states*

We stated in previous sections that dissipative and nonlinear terms in our model are of the same order of magnitude, that is

$$\omega \gg \Gamma \sim W\varepsilon^3 \sim WI^{3/2}.$$

It is of particular interest to consider the limiting case when we have maximal ratio of non-conservative to nonlinear terms while still permitting the stationary states to exist. Hereinafter we shall refer to these states as 'saturated'. In this limit the equilibrium phase is fixed (see (4.1))

$$\sin \Phi_0 = \pm 1. \tag{4.7}$$

The minus sign in (4.7) corresponds to generation of the central harmonic and dissipation of satellites, the opposite sign means the opposite energy balance. The exceptional nature of these saturated states lies in the fact that they have the minimal amplitudes $A, B$ at given $\Gamma_a$, $\Gamma_b$. They are the most 'non-conservative' equilibria and it is difficult to find their direct counterparts in the conservative problem. It is interesting to note that from the purely 'geometrical' viewpoint the saturated equilibria are those exhibiting the most curved and asymmetric fronts. We shall discuss some of their properties below.

## 4.2. *Linear stability of the equilibria*

In the previous subsection we found that the taking into account of non-conservative factors gives us a wide class of wave patterns of permanent form of quite different types. To select the physically meaningful ones we first consider the stability of the patterns.

The drastic difference in the characteristics of 'conservative' and 'non-conservative' equilibria at the first glance seemed to contradict to an intuitive understanding of the

weakly dissipative motion of a particle in a potential field. Indeed, the weak dissipative perturbation of one-dimensional potential motion can move slightly the coordinates of the stationary points; however the main qualitative features of this motion are evident: the particle moves near the stationary point losing its total energy and falling down into the potential hole (see figure 3), the centre just becomes the focus.

The principal point in our analysis of the stability problem is that the taking into account of non-conservative effects increases the dimension of the system due to the disappearance of the conservative integrals of motion. As it was noted above, the new degrees of freedom allow the system equilibria to drift far from their conservative locations in the phase space, however small the non-conservative effects are. Having found these new equilibria specified by (4.1), one can perform a linear stability analysis in the vicinity of these points in rather general form.

In a standard manner we arrive at the eigenvalue problem

$$\det(\lambda \boldsymbol{E} + \boldsymbol{D}) = 0, \tag{4.8}$$

where the matrix $\boldsymbol{D}$ is

$$\boldsymbol{D} = \begin{vmatrix} -\Gamma_a & -\Gamma_a A_0/B_0 & 3WA_0^2B_0^2\cos\Phi_0 \\ -3\Gamma_b B_0/A_0 & 0 & -WBA_0^3\cos\Phi_0 \\ \Phi_a & \Phi_b & 3\Gamma_a + 2\Gamma_b \end{vmatrix}, \tag{4.9}$$

$\boldsymbol{E}$ is the unit matrix and

$$\left.\begin{aligned} \Phi_a &= (6V_{aaaa} - 8V_{abab})A_0 + W(9B_0^2 - 6A_0^2)\cos\Phi_0, \\ \Phi_b &= (24V_{abab} - 4V_{bbbb} - 8V_{bcbc})B_0 + 18WA_0B_0\cos\Phi_0. \end{aligned}\right\} \tag{4.10}$$

In the problem (4.8) positive $\lambda$ corresponds to stability. The conditions of stationarity are used. The eigenvalue problem (4.9) can be easily analysed numerically for the generic case. However, in this paper we shall focus upon the two distinguished limiting cases of the balance of nonlinear and dissipation mechanisms in order to clarify the physical conditions when particular types of the three-dimensional patterns of permanent forms can prevail.

4.2.1. *Infinitesimal non-conservative perturbations*

First we consider the case of infinitely small non-conservative effects which allows an easy analytical treatment. The eigenvalue problem (4.8) can be analysed in this case by means of the simplest perturbation procedure.

As the zero approximation we let

$$\Gamma_a = \Gamma_b = 0$$

and get simple expressions for the eigenvalues at the zero-order approximation

$$\lambda_1^{(0)} = 0, \tag{4.11a}$$

$$\lambda_{2,3}^{(0)} = [\pm(3\Phi_a WA_0^2B_0^2 - \Phi_b WA_0B_0^3)]^{1/2}, \tag{4.11b}$$

where the signs plus/minus correspond to the in-phase/out-of-phase equilibria. The eigenvalues do not depend on dissipation rates but they are not the same as for the 'conservative' problem because of significant displacement of the stationary states themselves in the phase space. We can easily obtain simple criteria of stability in this approximation in terms of the interaction coefficients (see Appendix B). We note that instability criteria in this case are expressed in terms of wave amplitudes only and do not depend on non-conservative mechanisms. So, we can refer to this type of stability

as 'conservative'. The stable in-phase equilibria can exist at any wave steepness in contrast to out-of-phase states which have a threshold steepness of about 0.33. We emphasize the drastic decrease in the threshold wave steepness (more than two times) for these out-of-phase states compared to the 'truly conservative' equilibria of § 3.2.

Apart from the modified 'conservative' instability considered above there are new instabilities due to the dissipative terms in matrix $\boldsymbol{D}$ having growth rates of order of these terms. To complete the picture we give the formulae and the explicit stability criteria in Appendix B.

Regardless of the smallness of these instabilities it seems very useful to analyse some of their specific properties. The appearance of 'absolutely' (with respect to both strong 'conservative' and weak 'dissipative' instabilities) stable states mainly depends upon the type of energy balance. If the central harmonic is generated and the satellites dissipate the in-phase states are absolutely stable in the above defined sense (see B 5*a*) for waves steeper than 0.18.

While the absolutely stable in-phase states occur in a wide range of amplitude parameters, the corresponding stability criteria for the out-of-phase states (B 7*a*) are incompatible for realistic wave steepness regardless of the type of energy balance. Does this mean that the corresponding structures are of no physical importance? The answer in the general case is no. In fact a kind of *meta-stable* state is possible. The instability can develop in some directions in phase space, but be very weak in other directions. This is just the case for the problem under consideration.

Indeed, let us calculate the eigenvector $\boldsymbol{\xi} = (\xi_a, \xi_b, \xi_\Phi)$ (indices of components of this vector correspond to the variables of our problem) for the zero eigenvalue in our problem (4.11*a*). We found that its component $\xi_\Phi$ is zero in the zero-order approximation. In the further approximation this component becomes of the order of the dissipation/generation rates, while the first two components of the eigenvector are of the order of the nonlinear terms which is much greater in accordance with the adopted scaling (4.4). This means that the further corrections to the zero eigenvalue leading to the 'non-conservative' instability affect mainly the amplitude dynamics, but not the phase $\Phi$ evolution. The resulting wave pattern will preserve its phase characteristics for a much longer period than the amplitude ones. The corresponding case needs the same type of energy balance as the stable in-phase states: energy going into the central harmonic and satellites dissipating.

The domains of absolute stability, instability and meta-stability are depicted in figure 9, Appendix B. Qualitatively the effect of infinitesimal generation/dissipation upon stability can be briefly summarized as follows:

(*a*) The attractors (absolutely stable equilibria) are found for the realistic wave amplitudes. The attractors correspond to the in-phase states.

(*b*) The *meta-stable* equilibria corresponding to the saddle-type points with relatively large positive eigenvalues and infinitesimal negative ones are permitted to occur within the realistic range of parameters. Such equilibria will manifest themselves as the relatively long-lived wave patterns. Both in-phase and out-of-phase states might be meta-stable in the above defined sense.

(*c*) The specific type of energy balance, namely energy going into the central harmonic and from the satellites, is more favourable to the appearance of persistent patterns.

We have paid so much attention to the case of infinitesimal non-conservative perturbations because of the fundamental importance of the concepts of attractive and meta-stable equilibria we formulated. For these effects to become apparent in

finite time one should consider non-conservative terms of the order of the dominant nonlinear ones. Such a situation will be analysed below.

4.2.2. *Stability of saturated states*

Linear stability of the saturated patterns corresponding to $\Phi_0 = \pm\pi/2$ in (4.7) can be treated in a manner similar to that of the previous subsection. The eigenvalue problem (4.9) for this case reduces to the following extremely simple equation (see (4.8), (4.9)):

$$(\lambda + 3\Gamma_a + 2\Gamma_b)(\lambda^2 - \Gamma_a\lambda - 3\Gamma_a\Gamma_b) = 0. \tag{4.12}$$

Its solutions give us explicit stability criteria in terms of dissipation coefficients

$$\Gamma_a > 0, \tag{4.13a}$$

$$3\Gamma_a + 2\Gamma_b < 0, \tag{4.13b}$$

or wave amplitudes

$$\frac{B_0^2}{A_0^2} \leqslant \frac{2}{9}. \tag{4.14}$$

Condition (4.13*a*) means that stable saturated patterns are possible only if the input of energy goes into the central wave and the satellites are dissipating. It also selects the unique value of the phase $\Phi_0$ that, as will be shown below, prescribes uniquely the orientation of the wave fronts: the crescents are oriented forward.

Condition (4.13*b*) gives the most transparent form in terms of $\Gamma_a$, $\Gamma_b$:

$$|\Gamma_b| \geqslant \tfrac{3}{2}|\Gamma_a|. \tag{4.15}$$

This means that the dissipation decrement should exceed the generation increment. On reformulation in terms of wave amplitudes (4.14) it ensures the fact of principal importance – a limitation of the satellites' amplitude in the stable patterns.

### 4.3. *Discussion*

In §4.1 we first found a family of stationary three-dimensional waves and later in §4.2 identified the patterns which are absolutely stable with respect to linear perturbations. The absolute stability in the linear approximation guarantees just that all the trajectories are attracted into the chosen stationary point that are originated close to this point. The study of the global properties of the trajectories requires a quite different approach and goes beyond the scope of the present work. However just to see whether the domains of attraction in the phase space are large and are not confined to the vicinity of the stationary points found we performed a number of numerical simulations of system (2.19) choosing initial states in a random manner.

4.3.1. *Simulations*

The simulations indicate (in no way we are claiming that they prove) the following. The equilibria we found may have vast domains of attraction in the phase space in the case of the very large amplitudes. For the waves of small and moderate amplitudes the domains of attraction proved to be rather small. An example of the trajectories in the phase space in the vicinity of a saturated equilibrium is given in figure 6. For better illustration we took a large amplitude corresponding to steepness of about 0.35, although similar attractors are possible for the waves of moderate steepness of about 0.2 as well. The wave patterns corresponding to the limiting state of figure 6 are depicted in figure 7. Discussion of other aspects of the numerical simulation is the subject of a separate work and will be reported elsewhere.

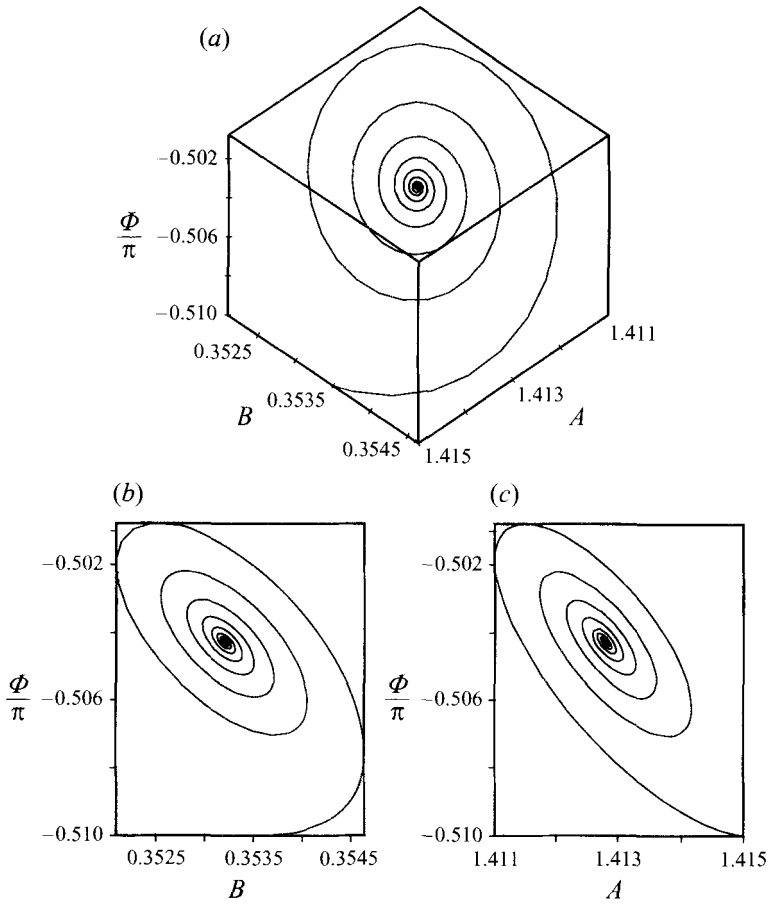


FIGURE 6. A typical scenario of the system evolution in the vicinity of the saturated state equilibrium. The wave steepness is about 0.35. (*a*) A trajectory in the three-dimensional phase space. (*b*, *c*) Projections on the planes $(A, \Phi)$, $(B, \Phi)$

4.3.2. *Front-back asymmetry*

It should be noted that the patterns given in figure 7 demonstrate noticeable *front-back asymmetry*: the maximal front slopes are steeper than the rear ones. We analysed a number of samples of stable equilibria with different parameters and found the same sign of such asymmetry everywhere. A common way to characterize the asymmetries of the random wave fields quantitatively is the use of some high-order odd statistical moments (see e.g. Elgar & Guza 1985). For the 'front-back' type asymmetry the most appropriate quantitative measure is (see Leykin *et al.* 1995)

$$\mathscr{A} = \langle (\hat{H}[\eta])^3 \rangle / \langle (\hat{H}[\eta])^2 \rangle^{3/2},$$

where $\langle \cdots \rangle$ is statistical averaging and $\hat{H}[\eta]$ is the Hilbert transform of the elevation function $\eta$. For all steady wave solutions of inviscid equations $\mathscr{A}$ is identically zero. The vanishing of $\mathscr{A}$ is due to specific properties of water wave nonlinear interactions which can only provide harmonics with a zero phase shift. The presence of either generation or dissipation changes the situation: the phase shift between the harmonics becomes of the order of the generation/dissipation. The positive $\mathscr{A}$ corresponds to steeper rear slopes, negative $\mathscr{A}$ means steeper fronts. We note that an interpretation

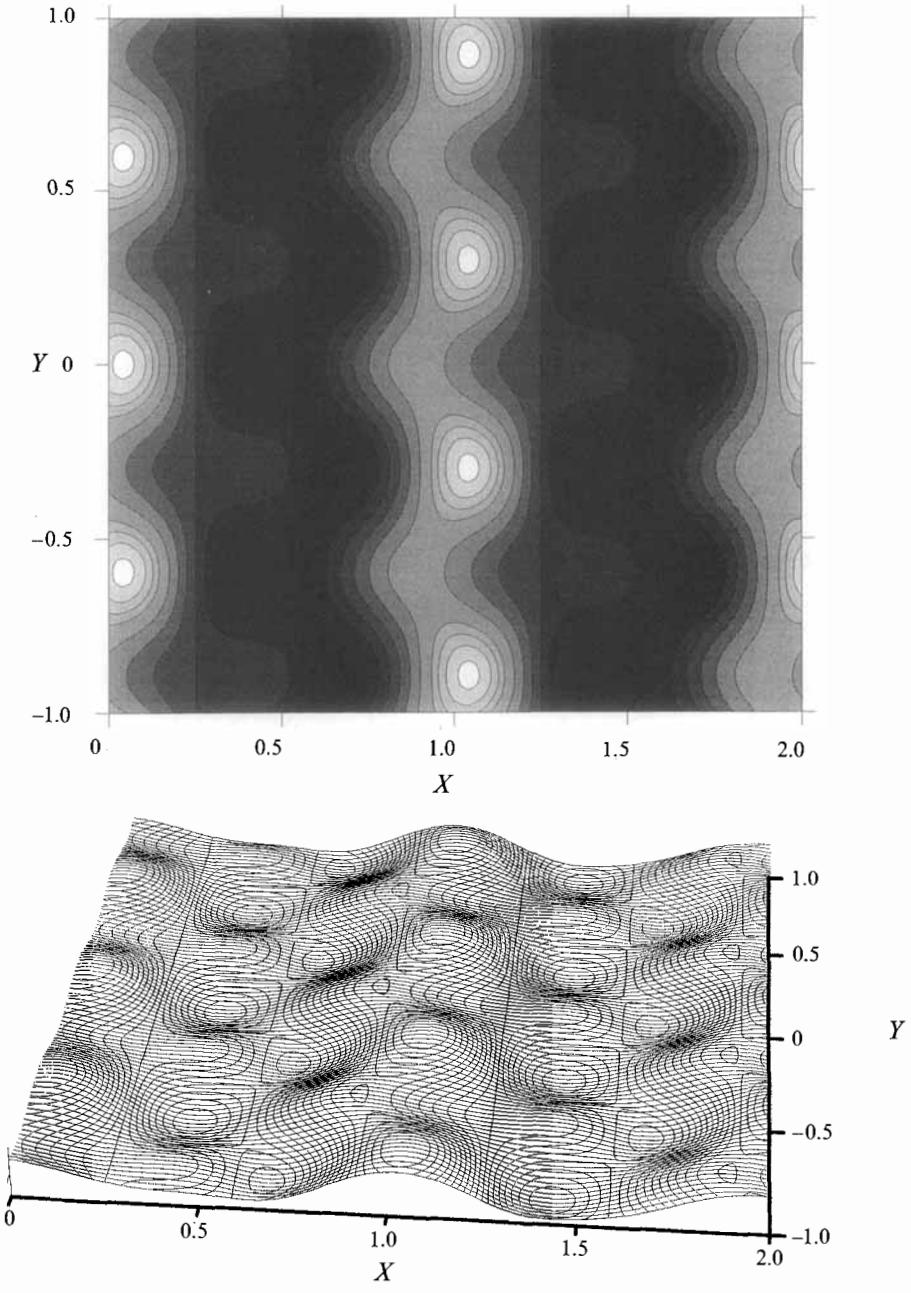


FIGURE 7. The saturated state pattern corresponding to the ultimate state of figure 6

of $\mathscr{A}$ as a quantity specified by interactions between the harmonics is common in the use of bi-spectral analysis (see e.g. Elgar & Guza 1985; Leykin *et al.* 1995).

We computed $\mathscr{A}$ for a number of patterns of steepness 0.25 with different phases $\Phi_0$ in the range $[0, -\pi]$. The asymmetry is negative in this range, it reaches its maximum in modulo, which is about 3%, at $\Phi_0 = -\pi/2$, i.e. at the saturated state. It is nearly zero for the in-phase and out-of-phase equilibria, which correspond to infinitesimal

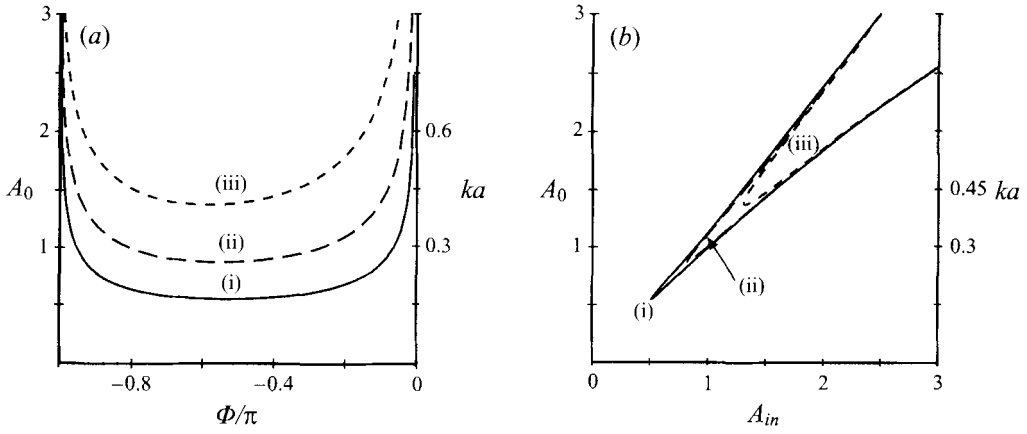


FIGURE 8. Equilibria *vs.* the 'initial' plane wave. The curves correspond to different dissipation/generation rates: (i) $\Gamma_a = 0.002$, $\Gamma_b = -0.001$; (ii) $\Gamma_a = 0.008$, $\Gamma_b = -0.004$; (iii) $\Gamma_a = 0.032$, $\Gamma_b = 0.016$. (*a*) The stationary state amplitude $A_0$ *vs.* the stationary state phase angle $\Phi$. (*b*) The stationary state amplitude $A_0$ *vs.* the amplitude of the 'initial' plane wave.

generation/dissipation. Thus the asymmetry, at least within our model, is a statistical measure of the ratio of non-conservative effects to nonlinearity. It is interesting to note that the maximal contributions into asymmetry are due to second-order terms, while those due to both the leading- and higher-order terms are usually noticeably smaller. The absolute values of $\mathscr{A}$ proved to be several times smaller than those available from the tank measurements by Leykin *et al.* (1995). The detailed analysis of asymmetry properties requires a special study.

We note that to our knowledge our solutions are the first *stationary* ones for waves of gravity range exhibiting the front-back asymmetry typical of the experimental patterns.†

### 4.3.3. *On the selection of ultimate equilibria through initial data*

The linear stability analysis allowed us to make a selection of the equilibria found. However based only on the stability analysis we cannot distinguish the most preferred states within the family of attracting equilibria. Being primarily interested in the equilibria resulting from the instability of a plane wave, we shall attempt to find the distinguished states by utilizing some additional assumptions on the initial stages of the instability.

We recall that for the given $\Gamma_a, \Gamma_b$ the equilibria within the family are specified by a single parameter, say the phase $\Phi_0$. The phase in its turn is fixed by the parameter of the linear frequency mismatch $\delta_{nc}$. The parameter $\delta_{nc}$ is an 'external' one for our system; it is formally prescribed by the initial selection of the main interacting modes comprising our system. The reasoning behind our choice of the particular three modes was based on the results of linear stability analysis for a plane wave. We chose the configuration that was maximally unstable within the linearized theory. Let us specify $\delta_{nc}$ so that for a given *initial* amplitude $A_{in}$ the mismatch provides maximal instability. Thus we can relate parameters $\delta_{nc}$ and $A_{in}$ and can express parameters of the equilibrium in terms of a hypothetical initial plane wave. Some of these dependencies are plotted in figure 8. Two three-dimensional steady patterns correspond to

† We note that the 'non-symmetric' stationary gravity waves derived by Zufiria (1987) do not describe this property. Roughtly Zufiria's solutions correspond to steadily propagating longitudinally modulated wave trains characterized by a non-symmetric distribution of the individual crests.

each initial plane wave. Figure 8(*a*) indicates the somewhat exceptional character of the saturated states. Indeed, depicting the dependence of the phase of an equilibrium on the amplitude of the initial plane wave under the given dissipation/generation, it clearly shows that the first transition from two- to three-dimensional waves (i.e. the transition occurring at minimal amplitude of the plane wave) selects the vicinity of the saturated state ($\Phi_0 = -\pi/2$). Although the valley is not sharp the effect is unambiguous. The dependence of the steady-state amplitudes on the initial amplitude in figure 8(*b*) illustrates this fact in a more expressive way: the minimal initial plane wave corresponds to the minimal amplitude of the three-dimensional structure in the vicinity of the saturated state. These arguments support the hypothesis that the saturated equilibria are the most distinguished ones in the following sense: if a plane wave evolves to an equilibrium owing to transverse instability and generation/dissipation it has more chance to reach the vicinity of the satuated steady state. We cannot prove this hypothesis now. Some additional arguments could be found in the fact that for the transverse instability to develop the plane wave should exceed a certain amplitude threshold, when dissipation of the satellites is taken into account. On the other hand to exclude breaking, the wave amplitudes should *not* exceed another threshold in the process of evolution. The requirement of compatibility of these restrictions gives a narrow gap between the initial and eventual amplitudes and thus selects the vicinity of the saturated states. At the moment, to provide more solid arguments in support of the hypothesis an extensive numerical simulation of the global properties of the trajectories seems to be the only available method.

## 5. Discussion

We shall discuss the results, focusing on the underlying assumptions. Some immediate implications will be briefly discussed as well.

We start with a brief summary of the main points. Our basic idea was that the experimentally observed three-dimensional patterns including the horse-shoe ones correspond to certain distinguished states of a comparatively simple low-dimensional dynamical system. To pursue this idea, we first selected a single triad noting that the fastest growing modes of the five-wave decay process (class II instability), being transversally symmetric, are phase locked with the central harmonic, thus allowing quasi-steady patterns. The analysis of the triad Hamiltonian dynamics leads us to the conclusion that at least within the framework of this system it is not possible to explain the emergence of any long-lived three-dimensional patterns. Taking into account the non-conservative effects makes the system dynamics richer. Owing to the loss of the conservative integrals the dimension of the system increases. In our context the principal new elements are as follows.

First, new three-dimensional equilibria appear that are essentially distinct from the conservative ones, however small the dissipation/generation.

Second, some of these equilibria are always attracting. The attracting equilibria in the parameter space were identified within the linear stability analysis.

Third, apart from the true attractors, meta-stable equilibria may appear. They are seen in the system dynamics as relatively long-lived patterns. The last step was the final selection of the 'most distinguished' steady state, based on some additional assumptions. The pattern which seems to be most likely to emerge from the class II instability of the Stokes wave is the limiting configuration of the allowed patterns corresponding to the minimal amplitude equilibria for the given dissipation/generation.

We called them the saturated states. These patterns do closely resemble the experimentally observed horse-shoes.

Let us discuss in more detail the reasons why we believe that the patterns provided by the theory are indeed the experimentally observed ones. The 'theoretical' horse-shoe patterns:

(*a*) can appear only for waves steeper than a certain threshold (about 0.2) and are characterized by relatively weak symmetric satellites;

(*b*) have flattened troughs and sharpened crests in the longitudinal cross-section;

(*c*) are front-back asymmetric: the front slopes are steeper than the rear ones;

(*d*) have asymmetric fronts: the fronts are crescent-shaped and always oriented forward.

Thus, the model well reproduces, at least qualitatively, all the main features of the horse-shoe phenomenon by now experimentally established. At first sight there is a difficulty in interpreting the Su (1982) tank experiments where there was no wind input. However the patterns observed by Su had a relatively short (in our $\varepsilon^{-3}$ scaling) time of existence. Most likely the Su patterns can be interpreted just as the manifestation of the first maximum of the satellite oscillations at the initial stage of a quasi-periodic regime similar to that described by Stiassnie & Shemer (1987).

It should be stressed that the model is aimed at providing just a qualitative description of the phenomenon. The extreme simplicity of the model brings not only advantages: it seems worth discussing again the main assumptions and limitations of the model.

In our opinion the most crude assumption is the selection of just three basic harmonics in Zakharov's variables and, in particular, neglect of the Benjamin–Feir modulation. Although there is experimental evidence that the modulational instability is suppressed by wind (Bliven, Huang & Long 1986), the principal question remains: what would happen if one considered many random harmonics subjected both to quintet and quartet interactions? Quite definitely the attractive equilibria we found will disappear. However it is possible that they may manifest themselves as some intermediate asymptotics. Say, if in the spirit of the Langevin approach we consider the evolution of our triplet with the interaction with the ambient wave field modelled by a random forcing, the system will tend to the old equilibria provided the domain of attraction is large enough. The main question of whether the attractors of the simple system we investigated would exhibit themselves in the realistic situations could be answered within such a model. The answer will depend only on the relative strength of attraction and random forcing due to all other interactions neglected in our model. In a favourable situation the system will often come into the vicinity of the old equilibria and the proportion of time it will stay there is considerable. Thus, this question could be in principle clarified by corresponding calculations and we may say that, at least, *a priori*, taking into account the realistic spectra of the wind-wave field and all their resonant interactions does not exclude manifestations of the attractors found, although in a somewhat modified manner.

The second assumption requiring discussion is concerned with the specific form of the generation/dissipation (linear ones) adopted in the model. We do not exclude that the dominant non-conservative mechanisms for the steep wave under consideration can become strongly nonlinear due to, say, airflow separation above the crests and microbreaking. It also possible that the leakage of energy into other modes due to neglected nonlinear interactions with the ambient field could provide nonlinear damping. At present we have neither a reliable theory nor a quantitative experiment to acquire nonlinear generation/dissipation to use in the model. How crucial is the

assumption of linearity? The answer varies for the different results. The very fact of the existence of an attractive equilibrium is the most robust, it depends only on the type of energy balance: whether the energy goes into the central wave and dissipates in the satellites or vice versa. The location of the equilibrium in the phase space is also robust, it is not sensitive to the particular type of amplitude dependence of the coefficients in contrast to the bounds of the domains of attraction, which are expected to be very sensitive. Thus, the existence of the stable equilibria found within our simplest model is meaningful, while the bounds of the domains of attraction, most likely, are not.

To get adequate wind input one should consider the self-consistent air–water problem: the airflow above waves is strongly affected by the three-dimensional steep sharp-crested patterns. This problem is among the first priorities of our further research. We note that one may expect the appearance of components of generation/dissipation phase-locked to the pattern. This type of non-conservative nonlinearity may result in especially non-trivial enrichment of the system dynamics.

The arguments in favour of the hypothesis on the distinguished character of saturated equilibria were fully discussed in §4.3.3. The seemingly good agreement with the experiment has not been quantified yet and, in itself, does not prove anything. The problem needs special consideration. We hope to clarify the mechanisms of the equilibria selection through numerical simulations in the near future.

Despite the number of open questions discussed above the principal fact of the existence of the horse-shoe patterns seems to be established and we can briefly discuss its most important implications.

The dominating basic concept of present-day study of wind waves is the idea that the wave field can be well represented by continuum of weakly interacting Fourier components with *random* phases, while the description of field dynamics in terms of its *statistical* characteristics, mainly temporal or spatial spectra, remains the prime goal of the mainstream studies. The presence of the coherent or phase-correlated structures in the wave field means non-Gaussian probability distribution, the obvious invalidity of the random phase approximation and, eventually, the inapplicability of the kinetic Boltzmann-type equations for the description of the field evolution for the scales under consideration. Some experimental evidence supporting this view based upon analysis of wave tank data was quite recently reported by Leykin *et al.* (1995).

In our opinion the presence of the three-dimensional sharp-crested coherent wave patterns should modify noticeably the drag characteristics of the sea surface and through this the air–sea momentum exchange. We also expect an important contribution of these structures to radar scattering at grazing angles. These issues are at the top of our agenda for further research. To progress in quantifying these claims the development of an essentially new model of the wave field allowing one to describe the coherent structures imbedded in the ambient noise is necessary, which is a quite formidable and challenging problem.

The tank experiments being conducted now at the large wind-wave facility of IRPHE-Luminy (Marseille) we hope will help to clarify many questions left unanswered by the present work.

The authors are pleased to thank Erik Mollo-Christensen for the photographs of the sea horse-shoe wave patterns he kindly provided for the paper. The authors are grateful to Sergei Annenkov and the referees, whose comments on the first version of the manuscript were very helpful. The work was supported by US Office of Naval Research (Grant N00014-94-1-0532), by INTAS (Grant No. 93-1373) and by International Science Foundation (Grants No. MMP000 and MMP300). V.S. and S.B.

are grateful for the hospitality of the Laborartory of Interaction of Ocean-Atmosphere of IRPHE, where part of the work was done.

## Appendix A. Relations among the canonical and physical variables

Canonical variables $a(\boldsymbol{k})$, $a^*(-\boldsymbol{k})$ are expressed in terms of Fourier amplitudes of surface velocity potential and surface displacement:

$$\eta(\boldsymbol{k}) = M(\boldsymbol{k})[a(\boldsymbol{k}) + a^*(-\boldsymbol{k})], \qquad \psi(\boldsymbol{k}) = -\mathrm{i}N(\boldsymbol{k})[a(\boldsymbol{k}) - a^*(-\boldsymbol{k})] \tag{A 1}$$

with

$$M(\boldsymbol{k}) = \left[\frac{|\boldsymbol{k}|}{2\omega(\boldsymbol{k})}\right]^{1/2}, \qquad N(\boldsymbol{k}) = \left[\frac{\omega(\boldsymbol{k})}{2|\boldsymbol{k}|}\right]^{1/2}, \tag{A 2}$$

where $\omega(\boldsymbol{k})$ is the dispersion relation of linear waves defined by

$$\omega(\boldsymbol{k}) = [g|\boldsymbol{k}|]^{1/2}$$

and

$$\eta(\boldsymbol{x}) = \frac{1}{2\pi}\int \eta(\boldsymbol{k})\mathrm{e}^{\mathrm{i}\boldsymbol{k}\cdot\boldsymbol{x}}\mathrm{d}\boldsymbol{k}, \qquad \eta(\boldsymbol{k}) = \eta^*(-\boldsymbol{k}), \tag{A 3}$$

$$\psi(\boldsymbol{x}) = \frac{1}{2\pi}\int \psi(\boldsymbol{k})\mathrm{e}^{\mathrm{i}\boldsymbol{k}\cdot\boldsymbol{x}}\mathrm{d}\boldsymbol{k}, \qquad \psi(\boldsymbol{k}) = \psi^*(-\boldsymbol{k}). \tag{A 4}$$

Here $\boldsymbol{k} = (k_x, k_y)$ is the horizontal wave vector, integration with respect to $\boldsymbol{k}$ is extended over the entire $\boldsymbol{k}$-plane, the asterisk denotes complex conjugate, and explicit dependence of $\eta$ and $\psi$ on $t$ is suppressed for simplicity of notation.

A canonical transformation to the new canonical variables $b(\boldsymbol{k})$, $b^*(\boldsymbol{k})$ is

$$\begin{aligned} a_0 = b_0 &+ \int A^{(1)}_{0,1,2} b_1 b_2 \delta_{0-1-2}\mathrm{d}\boldsymbol{k}_{12} \\ &+ \int A^{(2)}_{0,1,2} b_1^* b_2 \delta_{0+1-2}\mathrm{d}\boldsymbol{k}_{12} + \int A^{(3)}_{0,1,2} b_1^* b_2^* \delta_{0+1+2}\mathrm{d}\boldsymbol{k}_{12} \\ &+ \int B^{(1)}_{0,1,2,3} b_1 b_2 b_3 \delta_{0-1-2-3}\mathrm{d}\boldsymbol{k}_{123} + \int B^{(2)}_{0,1,2,3} b_1^* b_2 b_3 \delta_{0+1-2-3}\mathrm{d}\boldsymbol{k}_{123} \\ &+ \int B^{(3)}_{0,1,2,3} b_1^* b_2^* b_3 \delta_{0+1+2-3}\mathrm{d}\boldsymbol{k}_{123} + \int B^{(4)}_{0,1,2,3} b_1^* b_2^* b_3^* \delta_{0+1+2+3}\mathrm{d}\boldsymbol{k}_{123}. \end{aligned} \tag{A 5}$$

The arguments $\boldsymbol{k}_j$ in $a$, $\omega$, $U^{(n)}$, $V^{(n)}$ and $\delta$-functions are replaced by subscripts $j$, with the subscript zero assigned to $\boldsymbol{k}$. Thus, for example, $a_j = a(\boldsymbol{k}_j, t)$, $\omega_j = \omega(\boldsymbol{k}_j)$. The reduced 'five-wave' Hamiltonian is

$$\begin{aligned} H = &\int \omega_0 b_0^* b_0 \mathrm{d}\boldsymbol{k}_0 + \tfrac{1}{2}\int V_{0123} b_0^* b_1^* b_2 b_3 \delta_{0+1-2-3}\mathrm{d}\boldsymbol{k}_{0123} \\ &+ \int W_{01234}(b_0^* b_1^* b_2 b_3 b_4 + b_0 b_1 b_2^* b_3^* b_4^* \delta_{0+1-2-3-4}\mathrm{d}\boldsymbol{k}_{01234}. \end{aligned} \tag{A 6}$$

The expressions for kernels $V$ and $W$ can be found in Krasitskii (1994) and contain 'natural' symmetry conditions in the explicit form:

$$V_{0123} = V_{1023} = V_{0132} = V_{2301},$$
$$W_{01234} = W_{10234} = W_{01324} = W_{01423} = W_{01432}.$$

The surface elevation $\eta$ of three-wave pattern under consideration given by the three-delta-functions ansatz (2.4) in terms of $b_k$ has 37 items in the Stokes-like expansion

under accepted $o(\varepsilon^4)$ accuracy. Here we give the expression for the elevation, confining ourselves to an $(\varepsilon^2)$ approximation:

$$\eta = \frac{1}{2\pi}\Big\{ AM(\boldsymbol{a})\cos(\boldsymbol{ax}) + BM(\boldsymbol{b})[\cos(\boldsymbol{bx}-\beta)+\cos(\boldsymbol{cx}-\beta)] + A^2[A^{(1)}(2\boldsymbol{a},\boldsymbol{a},\boldsymbol{a}) + A^{(3)}(-2\boldsymbol{a},\boldsymbol{a},\boldsymbol{a})]\cos(2\boldsymbol{ax}) + AB[(A^{(1)}(\boldsymbol{a}+\boldsymbol{b},\boldsymbol{a},\boldsymbol{b}) + A^{(3)}(-\boldsymbol{a}-\boldsymbol{b},\boldsymbol{a},\boldsymbol{b})) (\cos((\boldsymbol{a}+\boldsymbol{b})\boldsymbol{x}-\beta)+\cos((\boldsymbol{a}+\boldsymbol{c})\boldsymbol{x}-\beta)) + A^{(2)}(\boldsymbol{a}-\boldsymbol{b},\boldsymbol{a},\boldsymbol{b})\cos(\beta)(\cos((\boldsymbol{a}-\boldsymbol{b})\boldsymbol{x})+\cos((\boldsymbol{a}-\boldsymbol{c})\boldsymbol{x}))] + B^2[(A^{(1)}(\boldsymbol{c}+\boldsymbol{b},\boldsymbol{c},\boldsymbol{b}) + A^{(3)}(-\boldsymbol{c}-\boldsymbol{b},\boldsymbol{c},\boldsymbol{b})) (\cos((\boldsymbol{c}+\boldsymbol{b})\boldsymbol{x}-\beta)+\cos((\boldsymbol{b}+\boldsymbol{c})\boldsymbol{x}-\beta)) + A^{(2)}(\boldsymbol{b}-\boldsymbol{c},\boldsymbol{c},\boldsymbol{b})\cos((\boldsymbol{c}-\boldsymbol{b})\boldsymbol{x})]\Big\}. \tag{A 7}$$

The coefficients $A^{(i)}, B^{(i)}$ for deep-water gravity waves could be found, e.g. in Badulin *et al.* (1995) and for finite depth gravity–capillary waves in Krasitskii (1994).

## Appendix B. Stability criteria for weakly non-conservative stationary states

### B.1. *'Conservative' instabilities of non-conservative equilibria*

Formula (4.11*b*) yields an explicit expression for the growth rates of 'conservative' instabilities. The condition of stability ($\lambda > 0$), which specifies the bounds of the instability domains, in terms of interaction coefficients takes the forms:

(i) for the *in-phase* equilibria ($\Phi_0 \approx 2m\pi, m = 0, \pm1, \pm2, \ldots$)

$$18V_{aaaa} - 48V_{abab} + 4V_{bbbb} + 8V_{bcbc} + W(9R-36)A_0 < 0, \tag{B 1a}$$

that, upon inserting the values of interaction coefficients for deep-water waves†, yields

$$(R-4)A_0 - 6.06 < 0; \tag{B 1b}$$

(ii) for the *out-of-phase* equilibria ( $\Phi_0 \approx (2m+1)\pi, m = 0, \pm1, \pm2, \ldots$)

$$18V_{aaaa} - 48V_{abab} + 4V_{bbbb} + 8V_{bcbc} - W(9R-36)A_0 > 0, \tag{B 2a}$$

which for the deep-water case reduces to

$$(R-4)A_0 + 6.06 < 0. \tag{B 2b}$$

The above inequalities for the in-phase equilibria are illustrated in figure 9 (see curve i).

### B.2. *'Non-conservative' instabilities*

The taking into account of the small non-conservative terms in the eigenvalue problem yields both a new branch of small unstable eigenvalues and corrections to the already found 'conservative' eigenvalues.

The first-order correction to the zero eigenvalue can be written as

$$\lambda_1^{(1)} = -6\Gamma_b \frac{\Phi_a A_0 B_0 + \Phi_b B_0^2}{3\Phi_a A_0 B_0 - \Phi_b A_0^2}. \tag{B 3}$$

† The interaction coefficients are known for fluid of arbitrary depth; however for simplicity only we confine ourselves to consideration of deep-water waves.

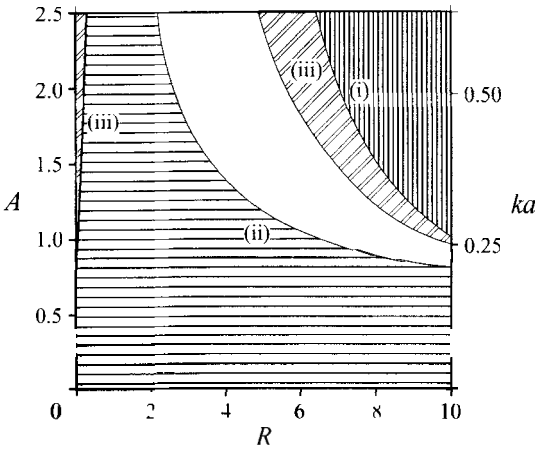


FIGURE 9. Stability diagram for the in-phase equilibria. (Case of generation of the central harmonic and the satellites dissipating.) (i) The 'conservative' instability domain is above the curve specified by inequality (B1*b*). (ii) The domain of 'purely non-conservative' instability prescribed by (B5) is below the curve. The whole domain below curve (ii) is meta-stable. (iii) Mixed instability domain is above the curves given by (B6)). The domain of absolute stability is unshaded.

It gives pure 'non-conservative' stability/instability.

The real value corrections to 'conservative' non-zero eigenvalues $\lambda_{2,3}^{(0)}$ can stimulate a mixed 'conservative-dissipative' instability

$$\lambda_{2,3}^{(1)} = \lambda_{2,3}^{(0)} + \Gamma_b \frac{3\Phi_a(R-2)A_0B_0 - \Phi_b(2R-1)A_0^2}{3\Phi_a A_0 B_0 - \Phi_b A_0^2}. \tag{B 4}$$

The 'pure non-conservative' stability for the in-phase equilibria ($\Phi_0 = 2\pi m$) yields

$$\Gamma_b \left[6V_{aaaa} - 8V_{abab} + (24V_{abab} - 4V_{bbbb} - 8V_{bcbc})R/3 + W(9R-6)A_0\right] > 0, \tag{B 5$a$}$$

that for deep water reads

$$\Gamma_b \left[(R-2/3)A_0 - 2.54 - 0.51R\right] > 0. \tag{B 5$b$}$$

The 'mixed' stability condition (real corrections to 'conservative' eigenvalues $\lambda_{2,3}^{(0)}$) gives

$$\Gamma_b \left[(24V_{abab} - 4V_{bbbb} - 8V_{bcbc} + (18V_{aaaa} - 24V_{abab})R + 9W(R^2 - 2R + 2)A_0\right] > 0, \tag{B 6$a$}$$

that for deep water results in

$$\Gamma_b \left[(R^2 - 2R + 2)A_0 - 7.61R - 1.54\right] < 0. \tag{B 6$b$}$$

For the out-of-phase stationary points ($\Phi_0 = (2\pi m + 1)$) the stability criteria can be expressed in a similar way The 'pure dissipative' stability is

$$\Gamma_b \left[6V_{aaaa} - 8V_{abab} + (24V_{abab} - 4V_{bbbb} - 8V_{bcbc})R/3 - W(9R-6)A_0\right] < 0 \tag{B 7$a$}$$

and

$$\Gamma_b \left[(R-2/3)A_0 + 2.54 + 0.51R\right] > 0. \tag{B 7$b$}$$

The 'mixed' stability (real corrections to 'conservative' eigenvalues $\lambda_{2,3}^{(0)}$) is

$$\Gamma_b \left[(24V_{abab} - 4V_{bbbb} - 8V_{bcbc} + (18V_{aaaa} - 24V_{abab})R - 9W(R^2 - 2R + 2)A_0\right] < 0 \tag{B 7$c$}$$

and

$$\Gamma_b \left[(R^2 - 2R + 2)A_0 + 7.61R + 1.54\right] < 0. \qquad \text{(B 7}d\text{)}$$

The set of the inequalities above specifies the domains of 'absolute', i.e. with respect to 'conservative' and 'dissipative instabilities'. The instability domains are plotted in figure 9.

The most crucial factor proved to be the type of energy balance. When energy enters the satellites and dissipates in the central harmonics the out-of-phase-state wave patterns proved to be always unstable, while stability of the in-phase equilibria is possible in a narrow parameter domain. Generation of the central wave and dissipation of the satellites, which is more realistic, allows wide class of the in-phase equilibria to be stable, while for the absolute stability of the out-of-phase states rather high amplitudes are necessary.

## REFERENCES


Badulin, S. I. & Shrira, V. I. 1996 On the Hamiltonian description of water wave instabilities. *Physica D* (submitted).

Badulin, S. I., Shrira, V. I., Kharif, C. & Ioualalen, M. 1995 On two approaches to the problem of instability of short-crested water waves. *J. Fluid Mech.* **303**, 297–325.

Belcher, S. & Hunt, J. C. R. 1993 Turbulent shear flow over slowly moving waves. *J. Fluid Mech.* **251**, 109–148.

Bliven, L. F., Huang, N. E. & Long, S. R. 1986 Experimental study of the influence of wind on Benjamin-Feir sideband instability. *J. Fluid Mech.* **162**, 237–260.

Craik, A. D. 1986 *Wave Interactions and Fluid Flows.* Cambridge University Press.

Elgar, S. & Guza, R. T. 1985 Observations of bispectra of shoaling surface gravity waves. *J. Fluid Mech.* **161**, 425–448.

Kharif, C. & Ramamonjiarisoa, A. 1990 On the stability of gravity waves on deep water. *J. Fluid Mech.* **218**, 163–170.

Krasitskii, V. P. 1990 Canonical transformation in a theory of weakly nonlinear waves with a nondecay dispersion law. *Sov. Phys. JETP* (Eng.transl.) **71(5)**, 921–927.

Krasitskii, V. P. 1994 On reduced Hamiltonian equations in the nonlinear theory of water surface waves. *J. Fluid Mech.* **272**, 1–20.

Kusaba, T. & Mitsuyasu, H. 1986 Nonlinear instability and evolution of steep water waves under wind action *Rep. Res. Inst. Appl. Mech. Kyushu University* **33**, No.101, 33–64.

Leykin, I. A., Donelan, M. A., Mellen, R. H. & McLaughlin, D. J. 1995 Asymmetry of wind waves studied in a laboratory tank. *Nonlinear Proc. Geophys.* **2**, No.3/4, 280–289.

McLean, J. W. 1982 Instabilities of finite-amplitude water waves. *J. Fluid Mech.* **114**, 315–330.

McLean, J., Ma, Y. C., Martin, D. V., Saffman, P. G. & Yuen, H. C. 1981 Three-dimensional instability of finite-amplitude water waves. *Phys. Rev. Lett.* **46**, 817–820.

Meiron, D. I., Saffman, P. G. & Yuen, H. C. 1982 Calculation of steady three-dimensional deep-water waves. *J. Fluid Mech.* **124**, 109–121.

Miles, J. 1994 Surface-wave generation revisited. *J. Fluid Mech.* **256**, 427–441.

Saffman, P. G. & Yuen, H. C. 1980 A new type of three-dimensional deep-water waves of permanent form. *J. Fluid Mech.* **101**, 797–808.

Saffman, P. G. & Yuen, H. C. 1985 Three-dimensional waves on deep water. *Advances in Nonlinear Waves* (ed. L. Debnath), Research Notes in Mathematics, vol. 111, pp. 1–30. Pitman.

Shemer, L. & L. Stiassnie, M. 1985 Initial instability and long-time evolution of Stokes waves. In *The Ocean Surface* (ed. Y. Toba & H. Mitsuyasu), pp. 51–57. D. Reidel.

Stiassnie, M. & Shemer, L. 1987 Energy computations for evolution of class I and II instabilities of Stokes waves. *J. Fluid Mech.* **174**, 299–312.

Su, M.-Y. 1982 Three- dimensional deep-water waves. Part I. Experimental measurements of skew and symmetric wave patterns. *J. Fluid Mech.* **124**, 73–108.

Su, M.-Y., Bergin, M., Marler, P. & Myrick, R. 1982 Experiments on non-linear instabilities and evolution of steep gravity-wave trains. *J. Fluid Mech.* **124**, 45–72.

WEILAND, J. & WILHELMSSON, H. 1977 *Coherent Non-linear Interaction of Waves in Plasmas.* Pergamon Press.

ZAKHAROV, V. E. 1968 Stability of periodic waves of finite amplitude on the surface of a deep fluid. *J. Appl. Mech. Tech. Phys. (USSR)* **9**, 86–94.

ZUFIRIA, J. A. 1987 Non-symmetric gravity waves on water of infinite depth. *J. Fluid Mech.* **181**, 17–39.